Supported Metal Pair-site Catalysts

Erjia Guan,[1#] Jim Ciston,[2] Simon R. Bare,[3] Ron C. Runnebaum,[1,4]

Alexander Katz,[5] Ambarish Kulkarni,[1] Coleman X. Kronawitter,[1] Bruce C. Gates[*1]*

1. Department of Chemical Engineering, University of California, Davis, California 95616, United States

2. National Center for Electron Microscopy Facility, Molecular Foundry, Lawrence Berkeley National Laboratory, Berkeley, California, 94720, United States

3. Stanford Synchrotron Radiation Lightsource, SLAC National Accelerator Laboratory, Menlo Park, California, 94025, United States

4. Department of Viticulture & Enology, University of California, Davis, California 95616, United States

5. Department of Chemical and Biomolecular Engineering, University of California, Berkeley, California 94720, United States

Current Address: Chevron Energy Technology Co., 100 Chevron Way, Richmond, California, 94804, United States

KEYWORDS supported metal catalysts, dinuclear catalysts, active sites, zeolites, X-ray absorption spectroscopy, CO FTIR, Scanning transmission electron microscopy

ABSTRACT

Complexes with neighboring metal centers and their analogues on surfaces are drawing increasing attention as catalysts. These include molecular homogeneous catalysts incorporating various ligands; enzymes; and solids that include pairs of metal atoms mounted on supports. Catalysts in this broad class are active for numerous reactions and offer unexplored opportunities to address challenging reactions, such as oxidation of methane and oxidation of water in artificial photosynthesis. The subject of supported metal pair-site catalysts is in its infancy, facing challenges in (a) precise synthesis, (b) structure determination at the atomic scale, and (c) stabilization in reactive atmospheres. In this Perspective, we summarize key characteristics of molecular and enzymatic catalysts that incorporate neighboring metal centers and build on this foundation to assess the emerging literature of metal pair-site catalysts on various supports. The supported catalysts include those synthesized by anchoring molecular dinuclear precursors to support surfaces and those synthesized by selective formation of dinuclear surface species from mononuclear surface species. Examples of metals in this class are rhodium and iridium, and

examples of supports are MgO and Fe_2O_3. We summarize characterization of these materials by electron microscopy and spectroscopy, emphasizing atomic-resolution aberration-corrected scanning transmission electron microscopy and spectroscopies that provide atomic-scale structural information and allow characterization of functioning catalysts, especially X-ray absorption spectroscopy. We list some opportunities for research, including suggestions that might lead to structurally well-defined supported metal pair-sites with new catalytic properties.

1. INTRODUCTION

Structures incorporating isolated metal centers are ubiquitous in catalysts—ranging from molecular transition metal complexes to enzymes to solid surfaces. Beyond catalysts incorporating single isolated metal atoms, catalysts that incorporate isolated pairs of metal atoms are gaining increasing recognition, because they have quite different properties and greater prospects for control of their properties. For example, many enzymes incorporate dinuclear metal centers, illustrated by those for methane conversion to methanol; the sites include dinuclear copper (sometimes with a third copper atom nearby), controlling electron transfer in catalysis.[1] Bioinspired homogeneous catalysts illustrate how incorporation of a second metal to create a heterobimetallic site offers opportunities to control the redox potential beyond what is possible just by changing organic ligand environments around one metal center—like those provided by amino acid residues near metal sites in metalloproteins.[2] Dinuclear metal complexes are good polymerization catalysts,[3] some with high activities and selectivities for copolymerization of epoxides and CO_2.[4] The activation of CO_2 benefits from bonding of one metal to the electron-rich

O atom and the other to the electron-deficient C atom, facilitating breaking of the metal–metal bond and formation of CO_2 bridging the metal atoms.

In a literature that is just emerging, pairs of metal centers on solid surfaces are being shown to have catalytic properties distinct from those of single isolated metal atoms and arrays of metal atoms on surfaces. Understanding of supported metal pair-site catalysts lags far behind understanding of molecular catalysts that incorporate pairs of metal sites. We posit that supported metal pair-site catalysts may offer significant new opportunities—and that understanding of molecular bimetallic catalysts may help advance the understanding of comparable multimetal catalysts on supports.

Our goal in this Perspective is to summarize the literature of supported metal pair-site catalysts: their synthesis, characterization, reactivity, and catalyst performance. We (a) compare them with catalysts having single, isolated metal centers; (b) offer insights about them based on comparisons with homogeneous and biological catalysts; and (c) provide suggestions for future research. Thus, we include a brief introduction to molecular and enzymatic catalysts that incorporate pairs of metal atoms.

The literature of supported metal pair-site catalysts is far less developed than that of supported metal single-site catalysts, which is one of the hot topics in catalysis research today.[5] Challenges in understanding catalysts in both of these classes are associated with (1) the difficulty of making them; (2) their heterogeneity—the nonuniformity of support surfaces and therefore the nonuniformity of species on the supports; (3) the smallness of the metal-containing structures that makes it difficult to identify them and their surroundings; (4) the lack of stability

of many of them; and (5) the complications associated with ligands that may help to stabilize the structures but are difficult to identify or even detect.

Synthesis is therefore central to this Perspective: investigations of supported metal pair-site catalysts benefit from precise synthesis to exclude species with metal nuclearities other than two—which, if present, confuse interpretations of characterization data and identifications of catalytically active species. Precise synthesis of catalysts in this class is challenging. The reported synthesis methods, summarized in detail below, include (a) reactions of molecular dinuclear precursors with supports to form anchored dinuclear precursors;[6] (b) controlled, selective aggregation of isolated single-site metals on supports;[7] and (c) synthesis and modification of supports to provide neighboring reactive sites for selective docking of metals in pairs or selective adsorption of single metal sites followed by selective bonding of a second metal on each of them.

Accurate, detailed structure determination is central to understanding these materials. Successful characterization requires combined methods, which we assess critically. Characterizations without atomic-resolution images of the metals may generally fall short. Such images are attainable for optimum combinations of metal and support, but images with sufficient resolution of metal atoms in pairs—in the absence of others—obtained by aberration-corrected scanning transmission electron microscopy (STEM)—are often challenging to obtain because the electron beam readily damages the structures.

We illustrate these points and emphasize the reactivities and catalytic properties of supported metal pair-sites. This essay is based on literature that is mostly recent and winnowed

for consideration of only *samples that consist almost entirely of clearly identified metal pair-sites*, and not mixtures. We begin with a foundation in molecular (homogeneous) catalysis.

2. MOLECULAR AND ENZYMATIC CATALYSTS WITH DINUCLEAR METAL SITES

The multidisciplinary subject of homogeneous metal pair-site catalysis has a history spanning more than four decades, assessed in comprehensive reviews,[8] It is a highly active area of ongoing research. The subject includes biocatalysis,[2] with numerous examples of cross-fertilization of these two subdisciplines of catalysis. Molecular catalysts incorporating two metals are called "bimetallic catalysts," whereas this term in heterogeneous catalysis refers to structures that incorporate two different metals, whatever the nuclearity or geometric arrangement of the metals.[9]

In 1982, the group of Muetterties[10] reported a seminal contribution to the field of homobimetallic catalytic hydrogenation. They used a bridged square-planar dimer comprising two adjacent rhodium centers (Figure 1) to catalyze stereoselective semi-hydrogenation of internal alkynes to the *trans* or (E)-isomers. The stereoselectivity differentiated this molecular catalyst from all those reported previously, which gave the *cis* or (Z)-isomer.[11] Such a single-step hydrogenation of an internal alkyne to give an (E)-alkene (without isomerization of the alkene product) is thought to be unattainable with a mononuclear active site, as the hydrogen transfer would need to occur from two different sides of the reactant molecule. Muetterties[11] originally hypothesized that a catalyst comprising two metal centers could circumvent this limitation through the formation of a bridged intermediate, to facilitate the stereoselective formation of an

(E)-alkene and dictate the stereochemical control in a manner that has no parallel for mononuclear metal complexes.

Muetterties's group characterized such an intermediate by single-crystal X-ray diffraction crystallography, finding it to consist of a bridged vinyl species that selectively forms upon reaction of the catalyst with an alkyne (but not olefins), even in the absence of hydrogen. This intermediate exhibits trans stereochemistry (thought to be controlled via sterics, Figure 1b) after reaction of the catalyst with di-*p*-tolylacetylene. This work is considered foundational in bimetallic homogeneous catalysis. Formation of an active site that consists of two metal centers acting cooperatively is now taken as a prerequisite for the direct synthesis (without alkene isomerization) of a *trans* (E)-alkene product resulting from the semi-hydrogenation of an internal alkyne, even when the resting state of the catalyst may be mononuclear.[12]

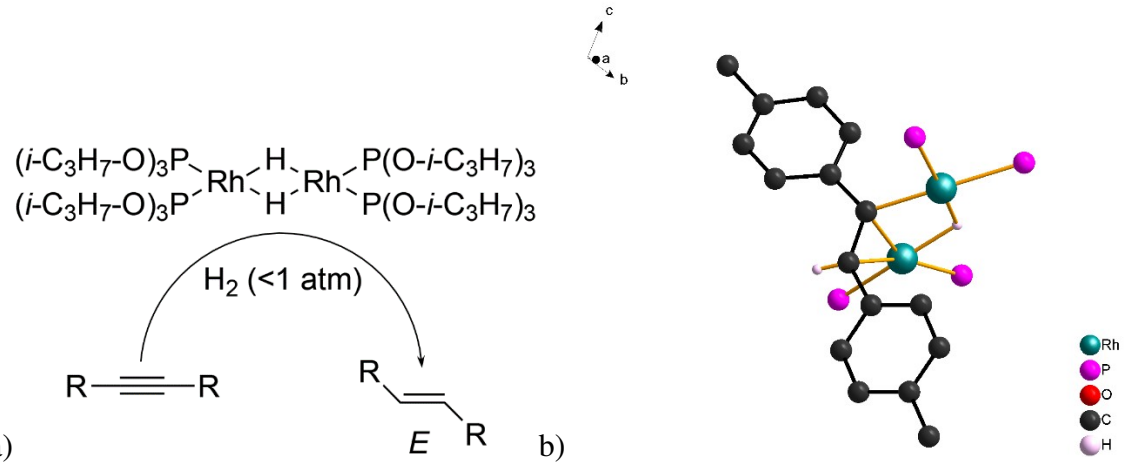

Figure 1. a) Muetterties's group discovered a di-rhodium catalyst that is active for selective semi-hydrogenation of alkynes to the *trans* or (E)-isomer. b) *Trans* stereochemistry is evident in the structure of the product of the reaction of the di-rhodium catalyst with di-*p*-tolylacetylene.

Panel a) is from reference,[10a] copyright (1982) American Chemical Society, and panel b) is from reference,[10b] copyright (1983) American Chemical Society.

The field of homogeneous pair-site catalysis has ballooned, now including illustrations of numerous heterobimetallic catalyst active-site architectures.[13] A current theme involves pairing of a transition metal as an electron donor with a nearby metal displaying Lewis acidity—to allow for dative charge transfer from the former to the latter. This type of interaction between two paired metals is common at the active sites of several metalloenzymes, with the dative bond often being established dynamically, during catalysis (akin to formation of a homobimetallic site during formation of the activated complex involving two mononuclear sites according to a recent report[12]), rather than in the catalyst resting state[2]. The dative bond in these catalysts enables tunability and control of metal redox potentials for catalysis over a much broader range than could be accessed with the typically available organic ligands (e.g., those with amino acid side chains—which already provide more than 0.5 V in redox potential tunability). This pair-site concept involving dative interactions has been implemented to explain the action of metalloenzymes with diverse catalytic functions, including nitrogen fixation and reduction/oxidation of organic molecules.[2]

We stress that much of the inspiration for this approach in *homogeneous* catalysis has arisen from concepts in *heterogeneous* catalysis, broadening our point about cross fertilization.[14] An example involves using a late catalytically active transition metal (e.g., a noble metal) on a support that incorporates an oxide of an early transition metal (e.g., TiO_2) with available empty d-orbitals for bonding with the former metal.[8c] The latter functions as a Lewis acid to accept

electron density from the former in the solid catalyst, presumably leading to enhanced catalytic activity via a metal–support interaction (i.e., charge transfer from the noble metal to the empty d orbitals of the early transition metal).[8d]

The homogeneous analogue of this type of construct is an "early/late" heterobimetallic catalyst.[13] There are several timely applications of such "early/late" paired metal sites, including those relevant to the activation of CO_2, as mentioned above.[15] Below we discuss recent work of the group of Thomas,[8d] because it links the systematic tuning of metal active site redox characteristics with this type of heterobimetallic construct for catalysis. Using heterobimetallic paired metal sites comprising a zirconium atom and a cobalt atom, the researchers inferred that the former acts as the Lewis acid, accepting electron density from the cobalt (Figure 2). The authors demonstrated the cobalt reduction potentials of the heterobimetallic complex to be nearly 1 V less negative than the reduction potentials of the comparative monometallic cobalt complex shown in Figure 2a. This difference translates to the ability to reduce cobalt under milder conditions as a result of the dative interactions between the two metals, suggesting that the reduction of organic reagents takes place under milder catalytic reaction conditions. This catalytic control is exemplified by data shown in Figure 2b, pertaining to activation (in Kumada coupling catalysis) of alkyl chloride reactants that are less reactive than alkyl bromides.[8c, 8d, 16] The homometallic cobalt catalyst is inactive, whereas the heterobimetallic zirconium-cobalt site is active (and both sites are catalytically competent for this reaction when the alkyl halides such as bromides are activated).

Another example involving homogeneous heterobimetallic catalysts for hydrogenation involves promoting the activity of earth-abundant nickel for hydrogen activation via dative bonding with a Lewis acid. Lu et al.[17] reported a nickel-gallium site that leads to the highest

hydride donating ability known for a nickel metal center—comparable to those of many noble-metal hydrides—and attributed to the Lewis acidity imparted by the neighboring gallium center in stabilizing an unusual anion, $[HNiGaL]^-$, and leading to an active catalyst for CO_2 hydrogenation at the heterobimetallic nickel-gallium site. In contrast, the monometallic gallium site with the same organic ligands is inactive.

In olefin hydrogenation catalysis, there are similar activity effects, as the monometallic nickel analogue was also found to be inactive for this reaction, with the nickel-gallium in contrast being active. There are also interesting selectivity effects: the nickel-gallium heterobimetallic site catalyzes only hydrogenation, without isomerization of terminal olefins with allylic protons to give internal olefins, whereas nickel-indium sites catalyze both reactions.[8e, 18]

Pointing to the future of pair-site catalysis, Muetterties stated: "reactions must await design of more robust, catalytically active coordinately unsaturated clusters."[19] We might suggest that some of these would be on solid surfaces that help stabilize the coordinative unsaturation.

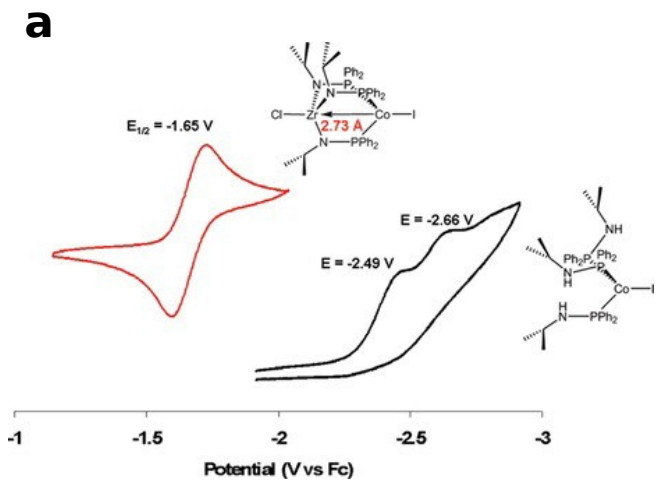

Figure 2. (a) Comparative cyclic voltammograms of zirconium-cobalt heterobimetallic and cobalt monometallic catalysts incorporating the same phosphinoamine ligands. Figure

reproduced from reference,[8d] copyright (2011) Taylor & Francis. (b) Comparative catalytic data characterizing the Kumada coupling reaction of alkyl halides and *n*-octylmagnesium bromide with the zirconium-cobalt heterobimetallic precatalyst and the cobalt monometallic precatalyst shown in (a). Data adapted from reference.[8d]

Thus, an emerging trend at the interface of homogeneous and heterogeneous catalysis is anchoring homogeneous heterobimetallic active sites onto solid supports. A recent contribution demonstrates the anchoring of a rhodium-gallium site (and, for comparison, its rhodium monometallic analogue) on the internal surface of the MOF NU-1000. The heterobimetallic catalyst was found to be a proficient and selective catalyst for the semihydrogenation of diphenylacetylene, whereas the monometallic catalyst under similar conditions fully hydrogenates the reactant to make bibenzyl. These results demonstrate differences in the bonding of internal alkyne reactants and selectivity for the two catalysts. Significantly, although both of the catalytic sites form insoluble oligomers when exposed to H_2 in solution, the MOF, with its enveloping pores, prevents bimolecular decomposition under the same conditions.[20] This result is similar to results observed for iridium pair-sites stabilized with bulky substituted calix-[4]-arene ligands (Figure 3b); these examples provide support for a synthesis-followed-by-anchoring methodology for preparing paired-metal active sites on solids (details follow).

We stress that lessons learned from the molecular pair-site catalysis literature demonstrate that the chemistry is in no sense trivial, and the roles of the two metals may be quite diverse. Thus, even when two metals are arranged to be close to each other at near-bonding distances, they often act independently of one another—with little to no synergy in catalysis.[21] Thus, we stress that in our preceding summary about hydrogenation and reactions involving

hydrogen, we summarized exceptions to this statement. Even in these exceptional circumstances, the exact molecular basis for the synergy that favors the paired-metal catalyst remains unobvious. Specifically, in cases for which the pairing of metals alters redox potential associated with a dative interaction (which can be elucidated on the basis of charge transfer effects), it remains unclear whether this is the only reason for catalytic rate enhancement at the heterobimetallic sites.

The phenomena are rooted in thermodynamics and the resting state of the site. Yet catalysis is dynamic. Open questions have to do with how the thermodynamics related to the site redox potential affects the kinetics—why are there such large differences when the heterobimetallic site is active for Kumada coupling with alkyl chloride reagents whereas the monometallic site is inactive in the reaction depicted in Figure 2? Does this difference have to do with activation of the reagents or is it a transition-state effect? What are the molecular mechanisms by which the redox potential change has such a large effect? Alternatively, are there other reasons for the catalytic enhancements that are indirectly related to the redox potential change, such as cooperativity in one of the kinetically significant steps involving the second metal atom? These questions remain outstanding.[8d]

When the Lewis acidic partner metal in a series of comparative heterobimetallic pairs is varied systematically, catalyst performance data show an optimum strength of Lewis acidity.[8e] Similar questions arise here, as to how such results can be used to understand the mechanisms of catalysis more deeply. Such questions form part of the opportunity to understand and design such catalysts and—we posit—comparable supported catalysts.

3. SYNTHESIS OF SUPPORTED METAL PAIR-SITES

3.1. Strategies for Synthesis of Supported Metal Pair-Sites. Dinuclear metal complexes may be regarded as the simplest forms of metal clusters, at least when they incorporate metal–metal bonds. Adsorption of such compounds on supports is the most direct method for synthesis of supported metal pair-site catalysts.[22] Selective syntheses require that the nuclearity of the precursor be retained after chemisorptive bonding of the metals (or at least one of them) to the support. The chemisorption may lead to ligand removal from the precursor and/or to replacement of ligands, with the support becoming a ligand. Attempts at such syntheses often lead to unselective adsorption, possibly including reactions that lead to changes in metal nuclearity. Many dinuclear precursors are relatively unstable, some being coordinatively unsaturated and tending to dissociate into mononuclear species and/or evolve into species with higher nuclearities upon reaction with a support.[23] Prediction of successful synthetic routes requires consideration of the reactivity of the metal, its ligands, and the support surface chemistry. Examples of catalysts made with this approach are presented below; so far, there are only a few.

An approach different from chemisorption of a dinuclear precursor involves controlled aggregation of isolated single-metal species on supports to make dinuclear species selectively (Figure 3a). This method is less straightforward than the former and likely, we suggest, quite limited in applicability, but in favorable circumstances it allows selective formation of samples containing metal pair-sites on supports, often with the benefit that syntheses of mononuclear precursors require only relatively straightforward wet chemistry.

Another approach in prospect involves the formation of metal pair-sites by the selective fragmentation of larger clusters. It has been reported that, in solution, $Rh_4(CO)_{12}$ transforms into

$Rh_2(CO)_8$ in the presence of high-pressure CO or at low temperatures.[24] However, analogous chemistry on supports has not been reported, and one would expect that it would be difficult to carry out selectively, as mixtures, even including larger clusters, would be expected to form readily.[25] We foresee a more likely prospect being solution synthesis and purification to form dinuclear precursors that could then be anchored. However, to repeat, such harnessing of wet chemical purification methods is useful only if there is a guarantee that the purified binuclear clusters remain intact following anchoring—otherwise, the benefit of the selective synthesis of the precursor might be lost.

Treatment of supports to create surfaces with sites or vacancies ready for selective anchoring metal pairs is another approach that is promising in prospect.

We illustrate these synthesis methods in the following section. We posit that many opportunities may emerge for synthesis of pair sites of a wide range of metals on a wide range of supports, even including zeotype materials,[26] as discussed below.

3.2. Examples of Synthesis of Supported Metal Pair-Sites. *Chemisorption of dinuclear precursors.* Among the synthesis methods, we suggest that the most general may emerge as that involving the direct anchoring of dinuclear organometallic species to supports, either intact or, more likely, with ligands removed (Figure 3b). These methods are expected typically to lead to metal–support bonding, perhaps with retention of metal–metal bonding.

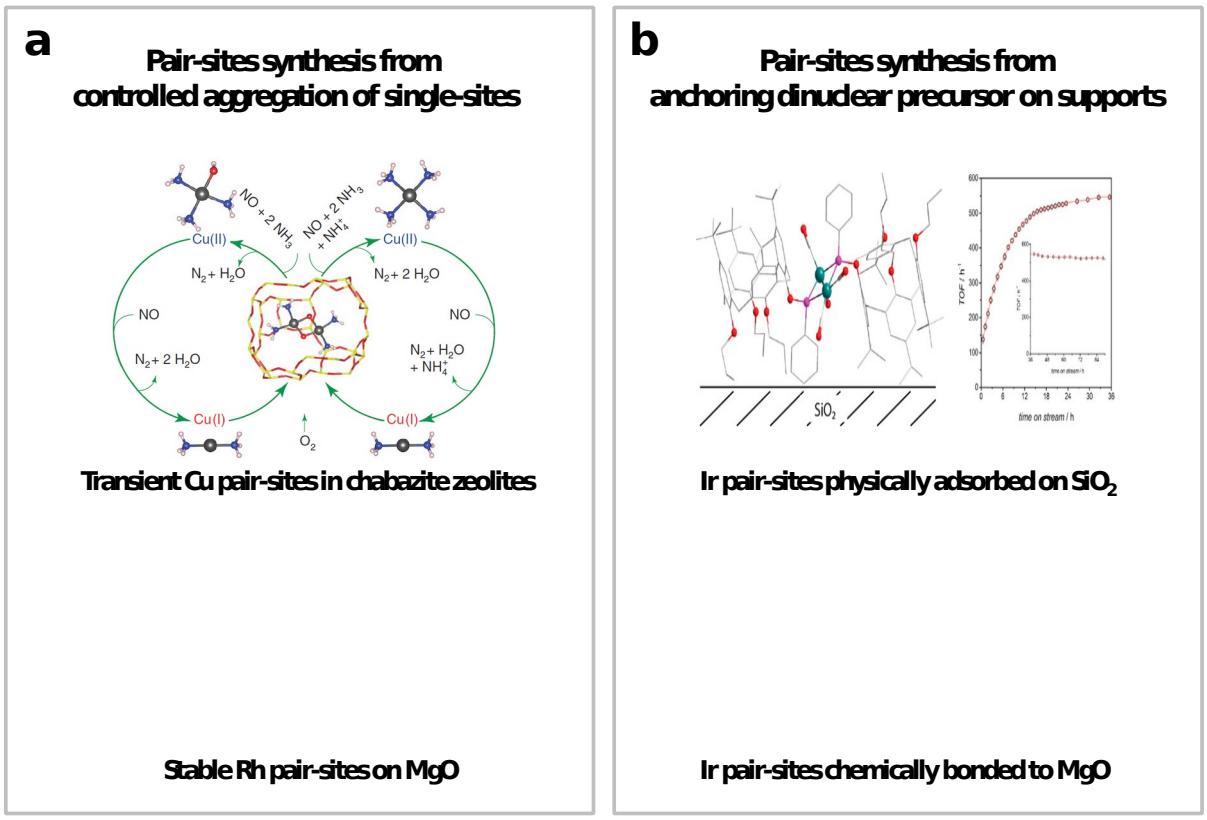

Figure 3. Schematic illustration of the synthesis of supported pair-site catalysts (a) by controlled aggregation of single-sites and (b) by anchoring of a dinuclear precursor onto the support. Panel a is a composite of figures, the upper part reproduced from reference,[27] copyright (2017) American Association for the Advancement of Science and the lower part from reference,[7a] copyright (2013) Wiley. Panel b is a composite of figures; the upper part is from reference[28] and the lower part from reference,[9a] copyright (2019) American Chemical Society.

To keep the precursor nuclearity intact upon adsorption on the support, bulky protective ligands may be helpful. For example, iridium pair-site catalysts incorporating phosphorus-bridging calix[4]arene ligands were found to be anchored (weakly) to silica when the precursor and support were slurried in an organic solvent.[28] The precursor remained essentially intact upon adsorption, with the bulky calix[4]arene ligands evidently protecting the dinuclear species from

aggregation during exposure to gases including ethylene and H_2 at 323 K and atmospheric pressure. In contrast to what was observed with iridium nanoparticles, no ethylidyne formed during exposure of the supported species to ethylene + H_2, as shown by the IR spectrum in the range of 2400–3800 cm^{-1} —the spectrum remained essentially identical to that observed as a result of the treatment in H_2.

More typically, however, dinuclear precursors undergo structural changes when reacting with a support. For example, the group of Iwasawa and Asakura[23] reported the preparation of rhodium pair-sites by the reaction of *trans*-[(RhCp*CH_3)$_2$(μ-CH_3)$_2$] (Cp* is pentamethylcyclopentadienyl) with silica. The precursor became weakly bonded to the support by losing approximately one methyl and one Cp* ligand, on average. Attempts to similarly graft the precursor onto other supports, such as on Al_2O_3 and MgO, resulted in break-up or aggregation of the metal-containing species.[23, 29]

In contrast, more stable rhodium and iridium pair-sites on MgO were synthesized by the reaction of $M_2(OCH_3)_2(COD)_2$ (M = Rh, Ir; COD = cyclooctadienyl) with partially dehydroxylated MgO (Figure 3b).[6a, 9a] The nuclearity of the precursor was retained after chemisorption on MgO, even under reactive atmospheres containing CO, H_2, or ethylene at temperatures up to 353 K. In the syntheses, one or two methoxy ligands on rhodium or iridium were replaced by bridging oxygen atoms that were part of the support surface, with the COD ligands remaining as protective ligands on the metal pairs. The M−M distances of the supported species were close to the distance between neighboring support oxygen atoms (~3 Å), as shown below in the sections about structure characterization. The metal–metal distances are respectively longer than the Rh–Rh and Ir–Ir bond distances of the precursors, but the neighboring metal

atoms were nonetheless found to be close enough to each other to cooperate during catalysis, as described in the section below about catalyst performance.

There is a parallel here with homogeneous homobimetallic catalytic sites involving ligand scaffolds that permit proximal placement of metals, sufficiently far apart that metal–metal bonds are not formed. In 1985, Bosnich et al.[21a] reported oxidative addition and reductive elimination reactions with such bimetallic active sites, concluding that oxidative addition on one metal prevented its occurring on the other nearby—interpreted to be the result of charge transfer from one metal to the nearby metal, resulting in formation of a metal–metal bond.

Changes in metal–metal distances as precursors accommodate to supports may be a rather general phenomenon. These examples show the importance of supports serving as templates to provide appropriate neighboring bonding sites for the metal pairs, but recall that, even in the absence of this metal pairing in the resting state, there can be dynamic changes during catalysis that alter metal–metal interactions, including bonding.

In another example, species with iridium pair-sites on α-Fe_2O_3 were synthesized by bringing the support in contact with a solution of an iridium homodimer bearing a bidentate 2-(2′ pyridyl)-2-propanolate (pyalc) ligand, $[Ir(pyalc)(H_2O)_2(\mu\text{-}O)]_2^{2+}$, followed by photochemical treatment.[30] After rinsing of the sample, stable iridium pair-sites were observed at neighboring threefold hollow sites on the α-Fe_2O_3 surface; details of the characterization of this sample follow in Section 4.1.

Formation of supported metal pair-sites from single-site metal species on supports. Numerous observations have shown that single-site metal species on supports are often not fixed in their initial locations.[31] In some cases, the metals migrate on the support surface, sometimes

even forming transient multinuclear intermediates under reaction conditions,[32] and often forming more stable metal clusters or nanoparticles. A broadly investigated example is multi-copper sites formed from isolated copper species in a zeolite.[27, 33] Details follow in Section 8.1.

Relatively stable rhodium pair sites on MgO powder were synthesized in high yield from single-site anchored $Rh(C_2H_4)_2$ complexes by exposure to H_2 at 353 K for 1 h at atmospheric pressure (Figure 3a), with no evidence of the formation of species having nuclearities higher than two.[7a] The electron-donating properties of MgO were suggested to be essential for the formation of stable rhodium pair-sites from the mononuclear precursor. In contrast to the electron-donating support MgO, electron-withdrawing (acidic) supports such as HY zeolite were found to favor the formation of larger rhodium clusters under the same hydrogenation conditions.[9b]

It remains to be understood why this preparation was selective for pair sites. It may be significant that DFT calculations[34] have shown that mononuclear iridium species on the strong electron-donor support MgO are more tightly bound than similar species on the less strong electron donor γ-Al_2O_3, and the former were correspondingly much more resistant to aggregation in H_2 than the latter.[34] However, these results do not explain why the metals in the pair sites were resistant to further aggregation. One could hypothesize that the pair sites were more stable than the isolated mononuclear metal species because they were coordinatively saturated 18-e^- structures whereas the mononuclear species were not. But this reasoning does not necessarily account for the observed stability of the pair sites during catalysis.[9b]

Selective atomic layer deposition has also been used to create pair sites, and the method may emerge as a promising synthesis method. A two-step synthesis involved modifying a

graphene surface to provide sites for selective docking of platinum in trimethyl(methylcyclopentadienyl)platinum(IV), and subsequent exposure of that sample to O_2 created sites where the platinum precursor reacted in another self-limiting reaction to make dimeric platinum in high yield on the graphene.[7b] Mild deposition conditions were required to avoid further metal aggregation.[7b]

It is clear that more research is needed to understand the conditions required for limited aggregation of single metal sites into pair-sites and to resolve the effects of thermodynamics and kinetics.

To summarize, we have listed in Table 1 synthetic methods used to prepare supported metal pair-site catalysts. Characterization methods are included in the table to provide links to following sections of this Perspective.

Table 1. Summary of syntheses and characterizations of some supported metal pair-site catalysts.

Metal pair/support	**Synthesis method**	**Methods for characterization of supported species**	**Nature of metal–support interactions**	**Ref.**
Rh_2/MgO	Controlled aggregation of single-site metal species	IR spectroscopy XAS	Chemisorption, often with metal bonded to support oxygen atoms	[7a]
Rh_2/MgO Ir_2/MgO Rh_2/SiO_2 Ir_2/SiO_2	Dinuclear precursor reacting with support in presence of a solvent followed by a solvent removal by evacuation	HAADF-STEM XAS IR spectroscopy NMR spectroscopy	Chemisorption or physisorption, depending on ligands and supports	[6a, 9a, 29]

			(details in main text)	
Cu_2/CHA zeolites[a]	Metal ion exchange on zeolites; pair-sites may form under reaction conditions, but see caveats below	XAS	Electrostatic interactions (details in main text)	[27]

[a]The copper pairs on zeolites are often transient and/or have non-uniform structures and nuclearities; see details below.

4. EXPERIMENTAL STRUCTURE CHARACTERIZATION

Definitive structural characterization of supported metal pair sites requires combinations of techniques; among the most valuable are the following:

- aberration-corrected scanning transmission electron microscopy (STEM) for imaging individual metal atoms and determining the degree of uniformity of the surface species;
- X-ray absorption spectroscopy (XAS) for determining average metal coordination environments and providing information about metal oxidation states;
- infrared (IR) spectroscopy for characterizing ligands on the metals; and
- density functional theory (DFT) for understanding the structures and predicting reactivities.

^{13}C and ^{1}H NMR spectroscopies are also powerful for characterizing the organic ligands in metal complexes on supports,[35] but there are barely any examples of dinuclear species characterized by

these methods, and we therefore provide no details here—but expect that the methods will become essential as the field emerges. We provide below brief summaries of characterization methods in addition to those in the list above.

In-situ and *in-operando* characterization techniques to track the structural changes of metal pair-sites during reaction and catalysis are important for understanding structure-catalytic activity relationships. In the following sections, we consider characterization of selected supported metal pair-site catalysts, with emphasis on those that have relatively well-defined structures. These prominently include rhodium and iridium pair-site catalysts. The reactivities and catalytic properties that set some of these samples apart from their single-metal-atom counterparts are discussed below, where we also mention opportunities for extending metal pair-site catalysts to planar and even single-crystal supports and zeolite cages.

4.1. Aberration-corrected STEM and Related Techniques. Aberration-corrected (AC) high-angle annular dark-field (HAADF) STEM imaging is a powerful technique for resolving oxide-supported heavy metal atoms with single-atom sensitivity; the sensitivity is attributed to contrast that scales approximately linearly in sample thickness and with the square of the atomic number of the imaged atom, in combination with atomic-scale probes and detectors exhibiting single-electron sensitivity. Thus, high-Z atoms (Z is atomic number) can be readily observed on thin, light-element supports with relatively straightforward interpretability. Although single-atomic catalytic species have been investigated extensively with this technique,[36] there are only a few examples pertaining to dinuclear species.[6b, 7b, 28, 32, 37]

The work of Zhao *et al.*[30] characterizing dinuclear iridium species supported on α-Fe_2O_3 clearly demonstrates both the strengths and limitations of this technique. Pairs of heavy iridium

atoms projected along the [001] and [241] zone axes of α-Fe_2O_3 were directly visible (Figure 4). However, because of the strong Z^2 scaling of the HAADF-STEM technique, it is not possible to directly image the presence or absence of Ir–O–Ir bridging species that are believed to be the catalytically active sites.

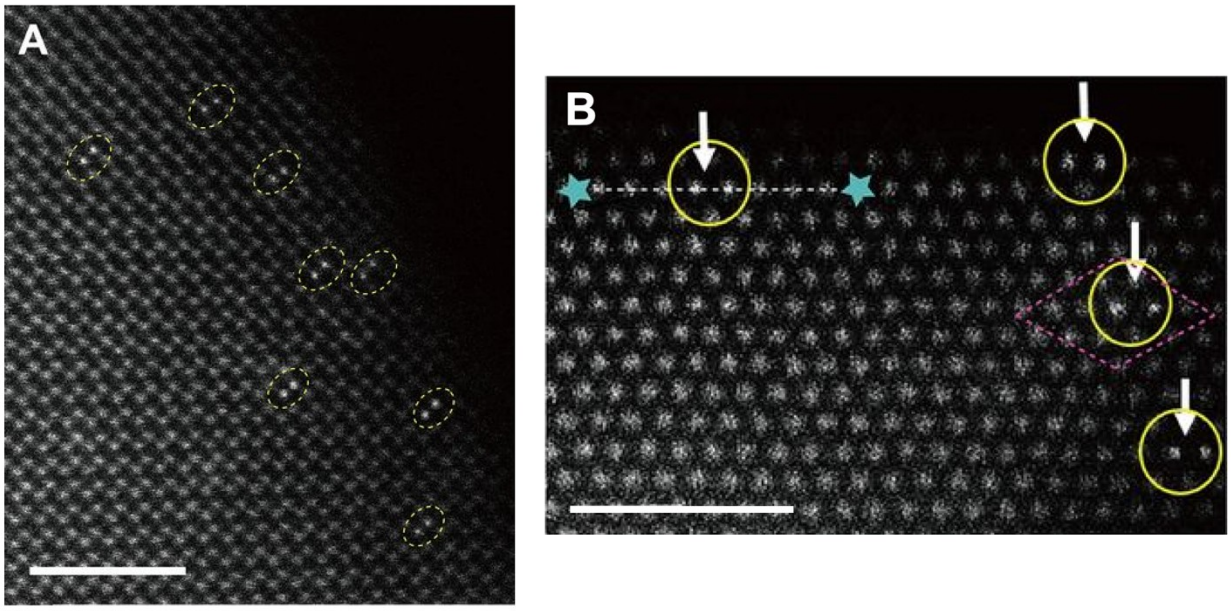

Figure 4. Observation by AC-HAADF-STEM of dinuclear iridium species supported on α-Fe_2O_3 as viewed along the (a) [243] zone axis and (b) [001] zone axes. Scale bars are 2 nm. Reproduced with permission from reference [30].

The presence of a bridging oxygen species in this example could only be inferred from the locally measured Ir–Ir distances determined by averaging the distance between bright spots on the linescan from the HAADF intensity analysis. DFT calculations (see below) and spectra determined by a nonlocalized surface-sensitive method and diffuse reflectance infrared Fourier transform spectroscopy (DRIFTS) data obtained with CO used as a probe provide additional indirect evidence of the local structures responsible for catalytic activity. As discussed in detail

below, XAS is a powerful method for determining the local bonding environments of the metal centers in these pair-site catalysts.[38]

This work motivates future research to attempt spectroscopic measurements of the local environments of dinuclear catalytic species using electron energy loss spectroscopy (EELS). AC-STEM-EELS has been used to detect monoatomic species of both heavy[39] (e.g., thorium, cerium, lanthanum) and light[40] (e.g., carbon, lithium) elements with sufficient fidelity to determine metal oxidation state and bonding information, as well as the presence of single lithium atoms,[41] and, recently, vibrational spectra of single silicon atoms.[42]

Although most single-atom EELS investigations have been performed with ultra-thin supports consisting of graphene and single-walled carbon nanotubes, calculations have shown that STEM-EELS and STEM-EDS (EDS is energy dispersive X-ray spectroscopy) should both be capable of identifying atoms in atomically dispersed supported metal catalysts.[43] AC-STEM is capable of both high resolution and high sensitivity, but the electron doses conventionally used for atomic resolution imaging are high, approaching 10^6 e^-/A^2 or more. These fluences can transfer significant energy to the adsorbed metals, such as iridium, leading to beam-induced sintering,[44] thereby complicating the interpretation of the native sizes of the metal-containing species. However, Ir–O–Ir species bound to α-Fe_2O_3 surfaces (Figure 4) were shown to be stable under AC-STEM illumination for a minute or more.[30] Inelastic transitions producing core-loss events that are sensitive to bonding effects for both oxygen and transition metal species by EELS are much rarer events than the thermally mediated scattering that produces HAADF contrast, increasing the potential for sample damage during EELS experiments.

It has recently been demonstrated that aberration-corrected high-resolution transmission electron microscopy (AC-HRTEM) can be used to directly image the dynamics of di-rhenium clusters within a single-walled carbon nanotube (SWNT) support (Figure 5A).[45] This investigation clearly demonstrates the effect of electron beam irradiation on CO ligands in supported $Re_2(CO)_{10}$ molecules, as shown by dynamic monitoring of the Re–Re distance from 0.30 nm in the $Re_2(CO)_{10}$ molecular cluster to 0.22 nm in the carbon-supported bare di-rhenium species (Figure 5B). That the electron beam served as both the imaging probe and the source of energy for dynamic decomposition of $Re_2(CO)_{10}$ highlights the challenges of using electron microscopy to provide atomic resolution insight in future *in-operando* investigations of catalysts consisting of metal pairs.

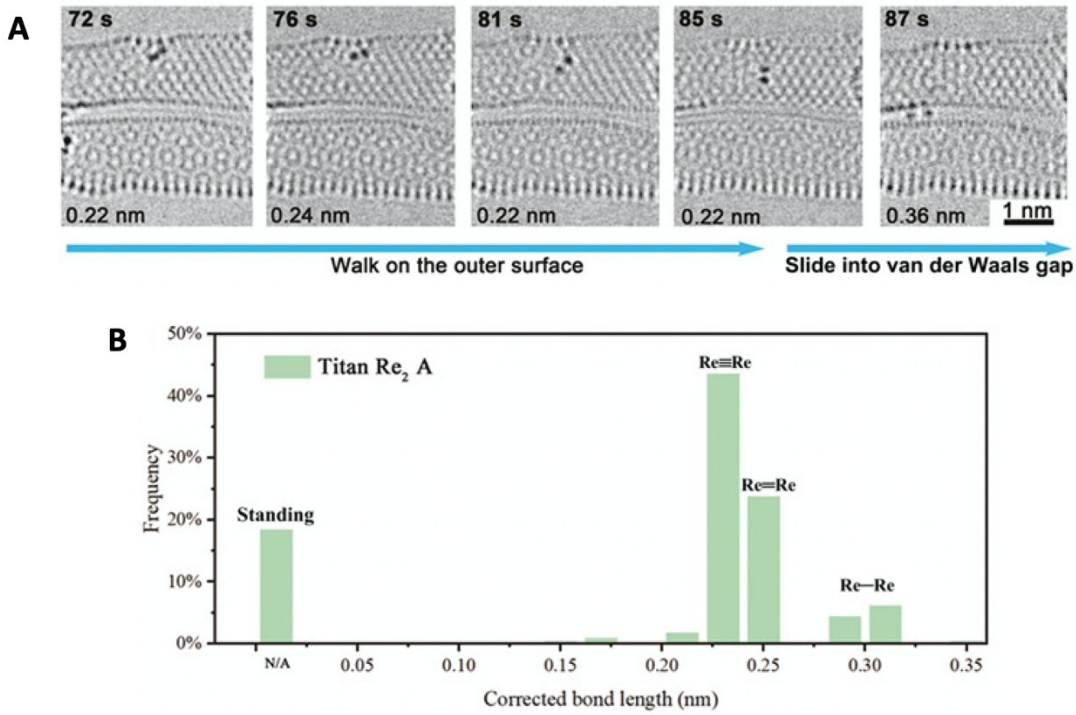

Figure 5: (A) Dynamic AC-HRTEM imaging of Re–Re atomic pair migration through a SWNT; (B) histogram of the observed Re–Re bonding distance, giving insight into the bonding

chemistry and indirect evidence of the density of CO ligands. Reproduced with permission from reference [45].

HRTEM has several potential advantages over the more commonly used HAADF-STEM technique when applied to beam-sensitive materials. The phase-contrast image formation mechanism can approach 50% efficiency with respect to the incident electron beam, which compares favorably with the 5–10% efficiency typical of HAADF- STEM and is associated with the relatively small fraction of electrons that are incoherently scattered to sufficient angles. As a full-frame imaging technique, HRTEM is also typically capable of greater temporal resolution than rastered STEM imaging, which can be a key metric for *in-situ* experimental investigations. The weak relationship between atomic number and phase contrast in HRTEM can allow for simultaneous imaging of heavy catalyst atoms and carbon- or oxygen-containing species on a support consisting of low-*Z* atoms. However, this constraint results in a much more challenging interpretation of images as compared with HAADF STEM and places much more stringent requirements on the maximum support thickness. Interpretability of HRTEM images is also challenged by the nonlinear nature of the phase contrast transfer function, which can vary significantly with the spatial frequency of the images with small changes in image focus.

4.2. X-ray Absorption Spectroscopy. X-ray absorption spectroscopy, which is often divided into two classes, X-ray absorption near edge structure (XANES) and extended X-ray absorption fine structure (EXAFS), is a powerful method for determining the local structures of samples such as those described here. It is element-specific and determines the number and type of nearest neighbors about an absorbing atom as well as interatomic distances, structural

disorder, and evidence of metal oxidation state. Furthermore, such information can be obtained *in-situ* or *in-operando*.[46]

XANES provides information about the electronic structure (empty local density of states), that is, oxidation state, and often local geometric structure, and it is broadly used in *in-situ/operando* experiments, offering the benefits of high sensitivity and quick response to changes in the electronic structures and coordination environments of the element being probed. For example, XANES spectra were used to monitor structural changes of iridium pair-sites on MgO during exposure to CO in a cell that was a flow reactor.[9a] As CO ligands gradually replaced the organic ligands on the iridium without changing the iridium nuclearity, an iridium edge position shift to higher energy was observed, showing that the oxidation state of the iridium changed as a result of ligand exchange. Isosbestic points were observed in the spectra recorded during the change, giving an evidence of a stoichiometrically simple transformation—in other words, mixtures with different iridium nuclearities did not form during the treatment.

XANES data are widely used, often in comparisons with the spectra of bulk reference compounds, as a basis for gaining information about oxidation states of metals in samples such as those described in this Perspective. XANES data often provide clear evidence of changes in metal oxidation states resulting from treatments, but the changes also reflect changes in the ligand sphere of the metal. XANES data are best used as a *guide* to the metal oxidation states and local symmetry, and, ideally, they are supported by theoretical calculations to aid in the interpretation.

Better bases for determination of structural models of supported metal species are provided by full analyses of EXAFS spectra. If EXAFS spectroscopy is to be used to characterize a metal pair-site catalyst, then it should be a prerequisite that the interpretation/modeling of the XAS data demonstrate that there is a signal corresponding to the metal–metal scattering path. This scattering path could either be a direct single-scattering metal–metal path at a bonding distance of the pair-site if it is a metal dimer, or a metal–bridge–metal single scattering path, if it is a bridged structure (e.g., M–O–M). Ideally, of course, if all the metal of interest in the catalyst were present in isolated dinuclear pair sites, then the coordination number of this scattering path should be unity. Similarly, if the dinuclear path is from a pair involving two different metals, then data would be presented for both metals (with the M_1–M_2 length being identical to the M_2–M_1 length) and provide a stronger demonstration of structure than would be available if the metals were the same.

An example is the work[9a] characterizing iridium pair-sites on MgO. The authors stated that their XAS data provide evidence of the iridium nuclearity, the bonding of the iridium to the MgO support, and the presence of the ligands bonded to the iridium. The Ir–Ir coordination number was determined to be 0.95 ± 0.2 at a distance of 2.99 ± 0.02 Å, which is a non-bonding distance, implying that the two iridium atoms were bridged by support oxygen atoms.

In comparison, although Yan et al. [7b] inferred that Pt_2 dimers were formed on a graphene support, using EXAFS to substantiate their claim, they did not explicitly provide either a model or data showing the contribution of a Pt–Pt scattering path to the XA spectrum, and thus a coordination number, or indeed an EXAFS-derived Pt–Pt bond length. Indeed, in the published peer review file accompanying the publication they stated “EXAFS simulations alone could not

draw the conclusion on the structures of the Pt_1 single atoms and Pt_2 dimers," and "excellent match between simulated curves and experimental data is not the purpose and could hardly be achieved by simulations, because there is no reiteration process to optimize the parameters such as interatomic distances, Debye-Waller factors, energy shift." For pair-site/dimer catalysts, surely, it is the distinction between single atoms and pair-sites/dimers that is the critical piece of information, and XAS has to be able to distinguish between these structures.

EXAFS spectroscopy strongly complements direct imaging of supported metals for structure determination. For example, the Ir–O–Ir structure inferred from STEM imaging (Figure 4) to exist on the Fe_2O_3 surface[30] was also characterized by EXAFS spectroscopy. Figure 6 shows the magnitude of the Fourier transform of the Ir L_{III}-edge EXAFS of the di-iridium complex. Yet in contrast with the remainder of the data in the report, which probes the iridium pair-site complex on Fe_2O_3, the XAS data were collected to characterize the complex supported on SBA-15, in the authors' words, to "avoid interference from the post-edge of the Fe signal from the α-Fe_2O_3 substrate, as well as the potential Ir–Fe scattering pathways." However, this caveat naturally casts some doubt on the relevance of the XAS data in support of the authors' claims of the pair site on the Fe_2O_3. The XAS data nicely show that the iridium is surrounded by six oxygen atoms at a distance of 2.02 Å. However, if the XAS data were being used to verify that an Ir–O–Ir complex existed, then such an Ir–O–Ir scattering path in the XAS data should be modeled. As shown in Figure 6, the authors modelled only the Ir–O scattering path and neglected an interpretation of the data in the 2.05–3.5 Å range that is evident in their data.

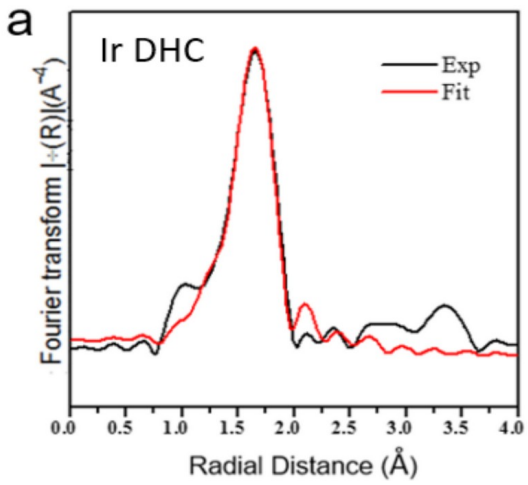

Figure 6. Magnitude of the Fourier transform of the Ir L_{III}-edge EXAFS for the Ir–O–Ir complex on SBA-15 and the best-fit model to the data. The data in the 2.05–3.5 Å range are not modeled. From reference [30].

A key piece of information to keep in mind in the interpretation of XAS data is that the resulting structure that is proposed is only a best-fit model to represent the data. Often researchers show results only for a best-fit model without clarifying what, if any, other models have been tried and how they compare with the one that is presented. It is preferable that multiple candidate models be presented. For example, Guan et al.,[9a, 6a] in the supporting information in their publications, showed several plausible models for their di-iridium and di-rhodium complexes on MgO and essentially left it to the reader to decide which is the most likely structure in each sample.

A best practice would be for authors to present their data in such a manner that the errors in the model and the statistical analysis are both shown and described to allow the reader to readily make a judgment on the merits of the models presented. Further, we stress that it is highly unlikely that XAS data alone will be sufficient to be conclusive regarding the unique

presence of a metal pair-site in a sample. For example, Guan et al.[9a] presented supporting structural information from STEM to substantiate the claims from XAS. In this case, for the di-iridium species on MgO, the Ir–Ir distance determined by STEM was found to be ~2.9 Å, in good agreement with the XAS-determined value; we return to this point below in the context of theoretical methods for modeling structures.

As discussed elsewhere in this Perspective, bulky ligands (e.g., calixarene phosphines) have been used to stabilize metal pair-sites in supported catalysts. A key question in these cases is whether the structure of the dimeric precursor, with the attached ligands, is preserved after adsorption on a support surface. Schöttle et al.[28] used XAS to ascertain whether the structure of the $[Ir(CO)_2PPhL]_2$ (L is the calixarene) was maintained on silica. In their XAS analysis, the authors used the known structure of the molecular complex to fix the coordination numbers of the numerous scattering paths in their XAS model and determined whether this model gave an acceptable fit of their data. This is an appropriate approach, but the results would have been more convincing if the authors had then let these parameters float and determined whether they converged on the expected values.

With EXAFS spectroscopy it is especially important to provide sufficient information regarding what part of the data is being modeled and, if not all of the data are being modeled, to provide some explanation of why a component of the data is not being modeled. For example, Tian et al.[9c] presented results characterizing a sample identified as a di-iron species supported on carbon nitride. They stated that their EXAFS data are consistent with an Fe–Fe scattering path at a bonding distance (2.43 Å) with a coordination number of 1.2. However, as shown in Figure 7, they neglected to discuss or model the clear intensity in the magnitude of the Fourier transform

(FT) of the data in the range between 3 and 5 Å. A comparison of the data characterizing the sample and those characterizing iron foil shows that the longer scattering paths in iron foil result in peaks in the FT in this same region, resulting in uncertainty about whether an appropriate model was used for the data.

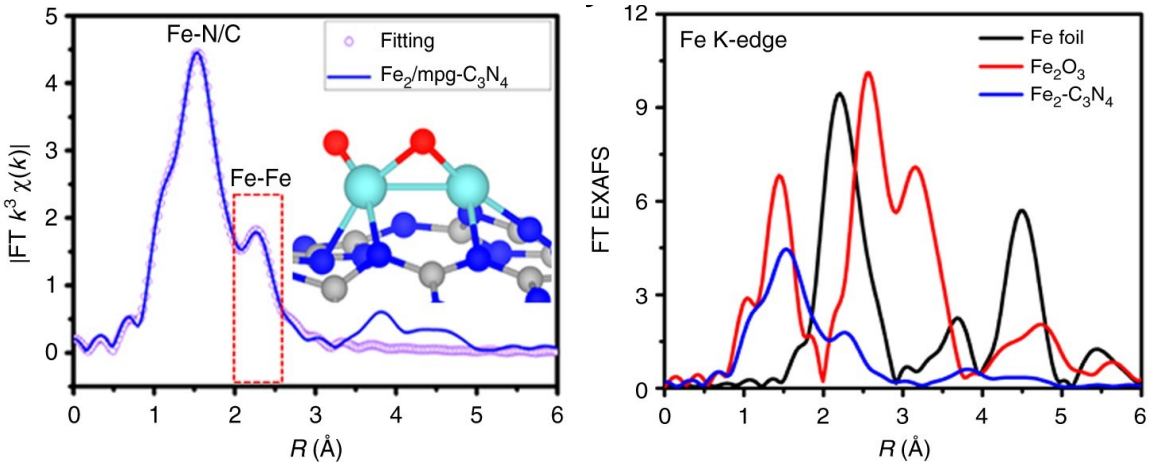

Figure 7. Comparison of the magnitude of the Fourier transform of the Fe_2/C_3N_4 catalyst with those of iron reference compounds. Note the similarity of the data in the range between 3 and 5 Å characterizing the catalyst and iron foil. From reference,[9c] copyright (2018) Springer Nature.

In electron microscopy, the impinging electron beam may cause the atoms to move, thus affecting the structure that is imaged. Similarly, in XAS the high-intensity X-ray beam can produce sample damage. However, this point is rarely mentioned in the XAS literature. One recommendation is that when XAS is used to validate a given structural motif, then there should be repeat experiments and mention of the reproducibility of the spectra as a function of data collection time.

4.3. IR Spectroscopy. IR spectroscopy is a valuable, typically inexpensive, technique for characterizing supported metal pair-sites by providing signatures of their ligands or the ligands

formed by addition of probe molecules. The spectra provide information not just about the ligands on the metals but—by inference—also about metal–support interactions and metal nuclearities, for example, through characterization of bridging ligands. IR spectra provide evidence of metal–support bonding by showing (a) shifts of characteristic bands of the non-support ligands on the metals and (b) changes in $\nu_{O\text{-}H}$ vibrations of support surface hydroxyl groups resulting from adsorption of precursors.

For example, the aforementioned silica-supported iridium pair-site catalysts that incorporate bulky P-bridging calix[4]arene ligands are characterized by IR spectra with CO band positions identical to those of the di-iridium precursor in hexane solution.[28] In contrast, the iridium pair-sites synthesized from $Ir_2(OCH_3)_2(COD)_2$ to give species chemically bonded to MgO were found to have C–H vibrational frequencies of COD ligands that were blue shifted by ~17 cm^{-1} as a result of adsorption of the precursor, reflecting a strong interaction between the metal and support.[9a]

The $\nu_{O\text{-}H}$ vibrations of support surface hydroxyl groups may provide evidence of the formation of metal–support bonds. For example, the formation of the aforementioned rhodium pair-sites and iridium pair-sites bonded to MgO was accompanied by a markedly decreased intensity (without a change in frequency) of IR bands of MgO surface hydroxyl groups as they reacted with the precursors.[6a, 9a] However, this method is limited when water is present or when abundant hydroxyl groups are present and hydrogen bonded to each other, causing broadening of the IR bands.

IR spectra also provide information about oxidation states of the metals and nuclearities of the metal species, usually on the basis of experiments with probe molecules, with CO being especially valuable.[47] Comparisons with DFT calculations are valuable, as described below. The CO stretching frequencies and the numbers of CO bands depend on the oxidation states of the metals and the nuclearity of the metal species. For example, $Rh(CO)_2$ supported on MgO (rhodium *gem*-dicarbonyl) through two Rh–O bonds is characterized by two ν_{CO} bands, at 2077 and 2000 cm^{-1}, representing symmetric and asymmetric vibrations of the terminal carbonyl ligands.[7a] Dinuclear rhodium carbonyls, $Rh_2(CO)_n$ ($n \approx 6$ or 7, depending on how the rhodium is bonded to the support) on MgO were characterized by 4 to 5 terminal ν_{CO} bands and two bridging ν_{CO} bands.[6a, 7a] The sharp, intense bridging carbonyl bands, at approximately 1850 and 1895 cm^{-1}, are characteristic of dimeric rhodium species on MgO, with the frequencies of these bridging CO bands being different from those characterizing bridging CO in larger (molecular) clusters such as $Rh_4(CO)_{12}$ or $Rh_6(CO)_{16}$.[48] Similarly, replacement of organic ligands with CO on iridium pair-sites on MgO led to the appearance of signature bridging CO bands at 1847 and 1883 cm^{-1}, as well as CO bands at higher wavenumbers representing terminal CO (Figure 8A).

The appearance of bridging CO bands upon exposure of a sample to CO may be a good indication of species with neighboring metal centers, but not all supported metal pair-sites form bridging CO ligands when exposed to CO. For example, reaction of CO with an MgO-supported species having strongly bonded acetate ligands, $Rh_2(OAc)_3$ (OAc = acetate), gave only weakly bonded CO on the open terminal sites on the rhodium centers, and the CO ligands were rapidly removed when the sample was exposed to flowing helium (Figure 8B).[6b] However, introducing

CO as a presumed probe molecule led to destruction of the original dinuclear structure by breaking of the metal–metal bonds and/or aggregation of the metal.[25]

The sharpness of the ν_{CO} bands provides information about the degree of uniformity of the supported pair-sites. For example, values of the full-width at half maximum (fwhm) of the bridging CO bands characterizing MgO-supported dinuclear species were found to be in the range of approximately 22–30 cm^{-1}.[9a, 49]

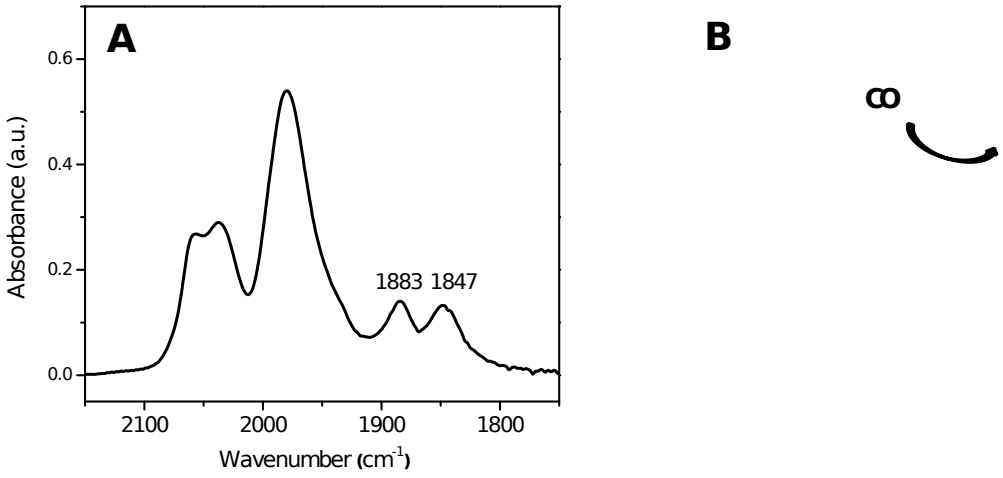

Figure 8. IR spectra in the ν_{CO} region characterizing the structures formed from (A) $Ir_2(\mu\text{-}OMe)_2(COD)_2$ on MgO after exposure to a CO pulse at 298 K for 3 min (schematic model: iridium (blue), oxygen (red), carbon (gray), magnesium (green)) and (B) $Rh(OAc)_3$ on MgO after exposure to a CO pulse at 298 K, then in flowing helium (model: rhodium (blue), oxygen (red), carbon (gray), hydrogen (light gray), magnesium (green)). (A) is from reference,[9a] copyright (2019) American Chemical Society, and (B) is from reference,[6b] copyright (2016) Elsevier.

4.4. Photoemission Spectroscopy. In addition to the essential techniques mentioned in Sections 4.1–4.3 (STEM, XAS, and probe molecule adsorption IR spectroscopy),

characterization by core-level photoemission spectroscopies is relevant to the goal of building a greater understanding of supported metal pair-site catalysts. X-ray photoelectron spectroscopy (XPS) is a core-level spectroscopy that provides information about the oxidation state and quantity of an element in the near-surface region of a sample. It is a ubiquitous method used for catalyst characterization, and with the advent of near-ambient-pressure XPS (NAP-XPS), measurements can be made *in-situ* or *in-operando*.[50] In the context of this Perspective, the most significant prior applications of photoemission have involved characterization of ligands and the oxidation states of the constituent metals in pair-sites, as well as supplementing traditional techniques for determining elemental composition. For example, Zhao et al.[30] used XPS to show that the ligands in the precursor used in their synthesis were absent from their supported iridium pair-site catalyst. As is common, in that investigation XPS was also used to confirm that there were no extraneous elements present following the synthesis of the supported di-iridium catalysts.

Data acquired from photoemission spectroscopies can potentially provide unique information regarding the nature of pair-site catalysts, as photoemission probes occupied electronic states, whereas XANES (Section 4.2) probes unoccupied states. In a recent example demonstrating the value of probing occupied electronic states in pair-site catalysts, atomically dispersed cationic platinum on CeO_2 was examined with synchrotron-based (resonant) photoemission spectroscopy in the context of H_2 dissociation.[51] In this investigation, it was determined that although supported Pt(II) species in a square-planar coordination (that is, the $Pt–O_4$ moiety) are inactive for H_2 dissociation, trace amounts of Pt(0) and oxygen vacancies in the support could result in charge transfer that activates isolated charged platinum for the reaction.

Given the importance of charge transfer in this activation mechanism, it is clear that photoemission techniques have the potential to play important roles in characterizing the nature of isolated metal pair-sites. As another simple example, when the bridged rhodium dimer precursor $Rh_2Cl_2(CO)_4$ was attached to a silica surface, XPS data readily indicated electron transfer from silica to the cluster, with associated reduction of Rh(I).[52]

Photoemission spectroscopies such as XPS are in general more readily accessible than XAS, and there has recently been increased availability of laboratory-scale high-resolution and NAP-XPS systems. Because of the complementary nature of data acquired through photoemission spectroscopy and XAS, the combination of these techniques can potentially facilitate unique contributions toward understanding the nature of isolated cationic sites and their associated catalytic activities. In the common situation wherein the metal constituents of pair-sites are bound to oxygen, the complementary nature of XANES and photoemission spectroscopy may be particularly valuable for characterization. For example, the electronic structure of CoO was analyzed in the context of a CoO_6^{10-} cluster model, with both multiplet coupling and Co 3d-O 2p hybridization taken into account to model Co 2p XA and XP spectra.[53] It was determined that features of the XPS data uniquely elucidated the mixed-valent nature of cobalt in CoO, and XANES data could be closely reproduced through simulated multiplet effects. Although detailed analyses comparing XA and XP spectra for pair-site samples have yet to be performed, the clearly demonstrated value of this combination for transition metal oxide systems implies that future investigations would benefit from the approach.

As a consequence of their lower output intensities, laboratory-scale XPS systems, in contrast to those used for photoemission spectroscopies at synchrotrons, require relatively high

metal loadings of samples for adequate characterization. Recent efforts toward increasing metal loadings while maintaining high metal dispersions on supports and site isolation are expected to lead to more applications of laboratory-scale XPS systems for characterization of metal pair-site catalysts.

4.5. Scanning Probe Techniques. Although a comprehensive summary is beyond this scope of this Perspective, it is relevant to acknowledge the vast literature of atomic-scale imaging of species by scanning probe techniques. Atomic-scale imaging of supported homo- and hetero-bimetallic dimers has historically been accomplished with model structures using scanning tunneling microscopy (STM) and atomic force microscopy (AFM), with the highest resolutions obtained in ultrahigh vacuum (UHV) and at cryogenic temperatures.[54] Indeed, the fine spatial manipulation afforded by scanning probes has enabled STM and atomic-resolution AFM to facilitate the direct synthesis of nanostructures with atomically precise structures and compositions.[55]

In a typical STM experiment designed to image clusters of surface-bound species with atomic resolution, adatoms are deposited onto single-crystal supports in UHV by evaporation and are imaged by quantifying current passed through an atomically sharp probe tip positioned sufficiently close to the electrically biased sample to facilitate electron tunneling through the vacuum gap. Many investigators have focused on imaging transition metal adatoms and their interactions on the surfaces of silicon crystals,[56] because of the relevance of these interactions to modern electronic devices and to the semiconductor industry generally. In many cases, dimers of adatoms were observed, as well as clusters comprising the deposited metal species and silicon atoms associated with silicon dimerization.

In especially stable samples, the local density of states can be assessed through scanning tunneling spectroscopy (STS), which facilitates inferences regarding the inter-atomic electronic interactions of the constituents of surface dimers, chains, and larger 2-D structures. As a representative example of the relevance of these methods toward understanding of pair-sites, isolated indium-tin and indium-indium dimers, as well as chains comprising these, were imaged by STM on atomically flat Si(001).[57] In this investigation, a combination of STS and the calculated local projected density of states was used to demonstrate that the local relative proximities of the dimeric species (and the associated charge transfer this facilitated) was determinative of whether the cluster could be characterized as metallic or semiconducting.

5. THEORY AND COMPUTATION FOR CHARACTERIZATION OF SUPPORTED METAL PAIR-SITES

Atomistic simulations, largely based on density functional theory (DFT), have been widely used for samples such as those described here to (1) provide structural information for comparisons with spectra (e.g., initial models being examined in fitting of EXAFS data, vibrational spectra, and metal–metal distances determined by HAADF-STEM imaging and EXAFS spectroscopy) and (2) provide insights into reaction mechanisms. Thus, computational methods have wide applicability and flexibility for investigation of this emerging class of catalysts.

Table 2 provides a brief summary of computational approaches, which are typically used in conjunction with experimental characterizations of metal pair-site catalysts. The most direct approach involves the comparison of DFT-optimized models with experimentally observed results (e.g., interatomic distances determined from micrographs) or experimentally inferred structure data (e.g., interatomic distances found by fitting of EXAFS data).

For example, Zhao et al.[30] used a DFT-optimized (PBE + U approach,[58] VASP software) structure to simulate the HAADF-STEM intensity (using Dr. Probe software) of their aforementioned sample incorporating iridium pair-sites on α-Fe_2O_3. Excellent agreement between the predicted and experimentally observed features (e.g., Ir–Ir distances of ~ 3 Å determined from linescans) provided strong evidence for the formation of a ligand-stabilized Ir–O–Ir motif on the α-Fe_2O_3 (001) facet.

The fact that heavier elements such as rhenium, rhodium, and iridium are more amenable to imaging by STEM than lighter elements presents an interesting challenge for DFT methods. Although the shortcomings of generalized gradient approximation (GGA) functionals for modeling highly correlated oxides is well-known in the heterogeneous catalysis community,[59] the challenges associated with modeling single heavy metal atoms (and, more challenging, pairs of heavy metal atoms) are better recognized in the domain of homogenous catalysis. These issues are related to the inherent accuracy and applicability of DFT methods, as discussed below.

Notwithstanding the limitations, one approach to characterize supported species is to screen a range of computational protocols (e.g., DFT functionals, U_{eff} values,[60] basis-sets, effective core potentials, etc.) to identify a method that provides sufficient agreement with experiments. For example, Cao et al.[61] screened a variety of functionals (e.g., PBE, BLYP, and M06-L), effective core potentials (e.g., LANL2DZ, SRSC), and basis sets (def2-SVP, def-TZVP) and concluded that BLYP/SRSC provided the best match with the results of their AC-HRTEM experiments characterizing their supported rhenium sample. A seemingly more accurate B3LYP hybrid functional was rejected because did not predict the multiplicity of the rhenium dimer ground state. Although screening of various computational protocols will lead to varying degrees of success (depending on the sample), the results of this investigation show how learnings from

high-level wavefunction methods (e.g., CASSCF/CASPT2 predictions of rhenium dimers[62]) can be applied for dimers of other metals on various supports.

Within the realm of metal pair-site catalysts, computational investigations are advantageous because they allow testing of specific hypotheses related to the ligand environments of the metals. For example, Guan et al.[9a] synthesized the previously mentioned iridium pair-sites using a dinuclear organoiridium precursor and used DFT-optimized models to interrogate the nature of the bonding between iridium atoms and the MgO support. By systematically examining modes of $Ir_2(COD)_2$/MgO and $Ir_2(X)_2(COD)_2$/MgO (where X = O, OH), they concluded that only the optimized $Ir_2(O)_2(COD)_2$/MgO structure agrees satisfactorily with their EXAFS data (Table 2). Although quantitative agreement between the Ir–Ir distance (~ 6% underestimated by DFT) and the Ir–O bond length (~ 2.5% overestimated by DFT) was not obtained even for the best model, the other models with different Mg–[X]–Ir interactions were significantly worse. Given the diverse ligand environments that are possible, we infer that such hypothesis-driven computer testing is likely to play an increasingly important role in determining structures of supported metal pair-site catalysts.

As support surface hydroxyl groups commonly constitute the binding sites for organometallic precursors of highly dispersed supported metal catalysts, it is necessary account for the correct coverage of the support surface in DFT models. This point is illustrated by the work of Zhao et al.,[30] whereby a hydroxyl-terminated α-$Fe_2O_3(001)$ surface (stable in the presence of water) was used for modeling their iridium pair-sites. The DFT-calculated Ir–O bond distance (2.05–2.15 Å) (as well as the coordination numbers) agrees well with the corresponding value determined by EXAFS data fitting (2.02 Å). This investigation highlights the importance

of including the appropriate reaction environment (e.g., a water atmosphere) for simulating high-valent atoms.

Although the point was not discussed in the publication, we posit that a discussion related to the changes in surface coverages by the relevant ligands (e.g., =O, -OH, and H_2O) for the pair-site catalyst, as a function of chemical potential (e.g., μ_{H2O}, which accounts for temperature and partial pressures), would be highly beneficial for future investigations. For example, the computational hydrogen electrode (CHE) approach[63] is commonly used for electrocatalysis and therefore readily applicable for similar reactions involving metal pair-site catalysts.

Building on the above discussion and given the simplicity of including harmonic free energy corrections for surface-bound ligands, we encourage the community to present surface phase diagrams in their reports. Notwithstanding the shortcomings of not including anharmonicity, such phase diagrams can provide crucial information about the state of the metal pair-sites in various oxidizing (or reducing) environments. Such surface phase diagrams are expected to prove useful for interpretation of experimental results (e.g., operando XAS, when the local surface environment may be dynamic).

Among the techniques that focus on structural information, the interaction of probe molecules such as CO characterized by IR spectroscopy is prominent among those supported by DFT calculations. A routine analysis involves comparing the harmonic CO vibrational frequencies with the band positions found experimentally. As with most DFT predictions, the calculated harmonic vibrational frequency depends strongly on the choice of the DFT functional. A common approach, especially within the wave-function and cluster modeling community, is to scale the calculated CO frequency on the basis of a known gas-phase reference.[64] This procedure was applied, for example, in modeling the aforementioned iridium pair-sites on MgO. The

authors[9a] showed that the vibrational frequencies characterizing the bridging CO ligands were underestimated, whereas the lower frequencies characterizing terminal-bound CO were overestimated. Although this analysis is complicated by the presence of multiple adsorbed CO molecules (the structure is approximated as $Ir_2(CO)_6$), the predicted vibrational frequencies are in satisfactory agreement with experiment. Similar agreement with experiment was observed by Zhao et al., for dinuclear iridium sites supported on WO_3.[65]

In addition to the effect of the choice of functional (likely adjusted by appropriate scaling[64]), the disagreement may arise as a consequence of the anharmonicity of some vibrational modes.[66] This point is likely true for metal pair-site catalysts, with a species such as a metal dimer being more flexible than the oxide support.[67] When IR spectra of CO ligands on the metal are used as an indicator of the presence of paired metal sites (e.g., for 3-d metals, which are light and challenging to image), we propose that incorporating the effects of anharmonic vibrational models may be necessary.

Table 2. Experimental and theoretical characterizations of supported metal pair-sites.

Experimental Technique	**Sample**	**Property**	**Experimental result.**	**Theoretical result**	**Comment**	**Refs.**
HAADF-STEM	$Ir_2(COD)_2$/MgO	Ir–Ir spacing	2.9 Å	2.8 Å[a]		[9a]
	Ir_2/α-Fe_2O_3	Ir–Ir spacing	3 Å	3 Å[b]	Excellent agreement between simulated and experimental HAADF-STEM micrographs	[30]
AC-HRTEM	Re_2/SWNT	Re–Re bond (η^6 binding)	2.3 Å	2.2 Å[c]	A range of functionals and effective core potentials were screened to identify the best agreement with experiment. The electronic structure of Re–Re is highly challenging within the DFT framework.	[61]
EXAFS spectroscopy	Ir_2/α-Fe_2O_3	Ir–O	2.01 Å	1.98–2.13 Å[b]		[30]
	$Ir_2(COD)_2$MgO	Ir–Ir Ir–O	2.99 Å 1.99 Å	2.80 Å 2.04 Å	Multiple models were optimized in DFT to identify structures consistent with experiment. Similar results were presented for $Ir_2(CO)_6$/MgO models as well.	[9a]
CO IR/DRIFTS	$Ir_2(CO)_6$/MgO	CO vibrational frequency, ν_{CO}	Bridged: 1842, 1885 cm^{-1} Terminal: 1953, 1963, 2026, 2059 cm^{-1}	Bridged: 1748,1843 cm^{-1} Terminal: 1998, 2009, 2036, 2064 cm^{-1}	Vibrational frequencies for the bridging bands are underestimated, whereas lower-frequency terminal bands are overestimated. A scale factor of 0.954 was used. CO vibrational frequencies are highly sensitive to the choice of functional. Thus, trends in the adsorption	[9a]

					energies are a useful indicator of changes in bonding.[a]	

[a]Guan et al.,[9a] ωB97X-D functional as implemented in Gaussian16, $(MgO)_{25}$ cluster model was used; [b]Zhao et al.,[30] PBE + U approach;

[c]Cao et al.,[61] B3LYP functional with Grimme's D3BJ corrections, SRSC effective core potential, cluster model for SWNT.

6. REACTIVITIES AND CATALYTIC PROPERTIES OF METAL PAIR-SITES ON SUPPORTS

6.1. Increased Rates of H_2 Activation Induced by Neighboring Metal Centers. The activation (dissociation) of H_2 on transition metals has attracted attention in catalysis and surface science for decades, and investigations of such chemistry on atomically dispersed metal catalysts on supports are an emerging area of research. Supported single-site metal catalysts may have low activities for H_2 dissociation, at least in part because of the limited numbers of available bonding sites, especially when the metals are bonded to metal oxides that are good electron donors or have ligands that are strongly bonded to the metal.[68] Metal clusters or surfaces are typically more reactive for H_2 dissociation than single-site catalysts incorporating the same metal, as illustrated by results for palladium, rhodium, and iridium.[69]

The benefits of neighboring metal centers in this respect extend to supported metal pair-site catalysts. Rhodium and iridium pair-site catalysts on MgO were found to have an order of magnitude higher reactivity for H_2 dissociation than single-site rhodium and iridium catalysts, respectively, on MgO, as evidenced by the results of H−D exchange experiments indicated by the reaction of H_2 with D_2, monitored by the formation of HD and bolstered by monitoring of hydrogen spillover to the support by IR spectroscopy of the resulting OH and OD groups.[6a, 9a]

An apparent consequence of the reactivity boost to H_2 activation provided by a neighboring metal center extends to catalytic hydrogenation of ethylene, for which hydrogen adsorption and dissociation are essential steps.[70] Ligands on the metals may exert a significant influence on the reactivity. For example, iridium pair-sites present as $Ir_2(COD)_2$ on MgO have only low reactivity for H_2 dissociation, as sites for bonding of hydrogen are blocked, but after

mild hydrogenation to partially hydrogenate and remove these COD ligands and replace them with hydride ligands, the reactivity and catalytic activity for H-D exchange increased.[9a] Thus, as shown by mass spectra of the effluent product, the activated iridium pair-sites after mild hydrogenation gave an initial conversion of ~12% when exposed to flowing H_2 and D_2 at 1 bar and 298 K, which is higher than that observed with the pair-sites having bulky ligands (~7.1%). As a result of this activation, the steady-state catalytic the activity for ethylene hydrogenation with an ethylene:H_2 molar ratio of 1.0 at 1 bar and 298 K (measured as a turnover frequency, TOF, (mol of ethylene converted) × (mol of iridium × s)$^{-1}$) was 0.084 s^{-1}, ~56 times greater than that of the pair-sites with the bulky ligands (0.0015 s^{-1}).

Protective ligands on the one hand can limit sintering of metal species and provide long-term catalytic performance, as was observed by Schöttle et al.[28] in their investigation with iridium dimers on silica that were protected by bulky calixarenephosphine ligands. However, bulky ligands can limit access to open metal sites and inhibit catalysis. The example stated in preceding paragraph provides some preliminary insight into how to find a balance between catalyst activity and stability.

Comparisons of the catalytic activities of single-site and pair-site catalysts and small metal clusters are usually limited because the ligands on the metals (including the reaction intermediates) are not the same, and these ligands typically influence the rate of catalysis significantly.

6.2. Reduced Poisoning by CO when it is Bridge Bonded rather than Terminally Bonded. CO is a well-known inhibitor or poison for many transition metal catalysts, to which it

bonds strongly; the metals include rhodium, palladium, iridium, and platinum, for example. The poisoning by CO can be minimized by application of higher temperatures to weaken the strength of CO bonding to the metal or by diluting the active metals with those that are less active, such as copper, silver, or gold.[71] For example, isolated platinum atoms in a copper surface (a dilute alloy) have much more resistance to CO poisoning than platinum nanoparticles.[72] CO is a strong inhibitor or poison of most atomically dispersed noble metal catalysts supported on metal oxides (e.g., SiO_2, MgO, or Al_2O_3). Attempts to minimize the detriment of CO poisoning by raising the temperature often cause aggregation of the metals—hence destruction of single-site catalysts.

In contrast to atomically dispersed supported metal catalysts, supported metal pair-site catalysts show markedly reduced poisoning by CO—as bridging CO ligands are more reactive than terminally bonded CO ligands, so that they can be dissociated (desorbed) from the metal during catalysis, even at room temperature. This point is illustrated for rhodium pair-sites on MgO. Initially inhibited by CO, the rhodium in these pair sites catalyzed selective 1,3-butadiene hydrogenation at increasing rates in a flow reactor as bridging CO ligands (less strongly bonded than terminal CO ligands) gradually desorbed, with the selectivity maintained (Figure 9).[9b] Similar results were observed for iridium carbonyl pair-sites on MgO, with the activity for ethylene hydrogenation growing as bridging CO was replaced by the reactants at room temperature.[9a]

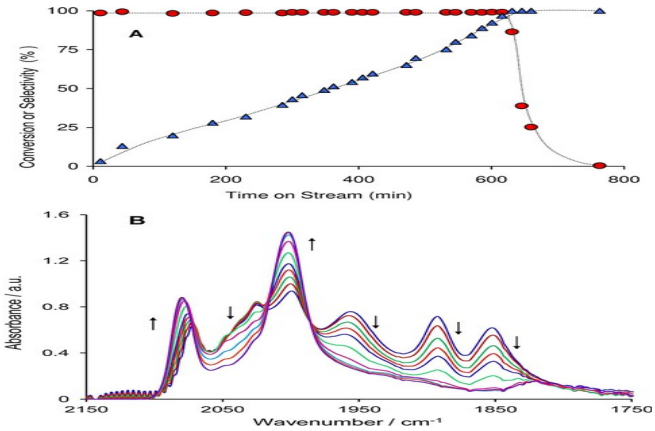

Figure 9. (A) Evolution of conversion (▲) and selectivity to *n*-butenes (○) in catalysis of 1,3-butadiene hydrogenation in a once-through flow reactor catalyzed by carbonylated rhodium clusters supported on MgO (reaction conditions: 313 K, 1 bar; total gas feed flow rate, 30 mL/min; feed component partial pressures, 20 mbar of C_4H_6, 980 mbar of H_2). (B) Time-resolved IR spectra in ν_{CO} region of the MgO-supported rhodium carbonyl clusters in a flowing mixture of 1,3-butadiene and H_2 at 313 K and 1 bar. Reproduced from reference,[9b] copyright (2016) American Chemical Society.

6.3. Multiple Bonding of Reactants for Selective Reactions. Neighboring metal centers allow multiple bonding of reactants either by bridging the neighboring metal sites and/or by bonding at two metal centers separately (see the examples of homogeneous catalysts mentioned above for homobimetallic rhodium sites for direct trans-semi-hydrogenation of internal alkynes or the ability to activate hydrogen in nickel-Lewis-acid-bimetallic pair sites). By tuning the ligands on the metals and opening specific bonding sites, pair-site catalysts have been tailored to offer high selectivities for reactions for which the comparable atomically dispersed single-site catalysts lack selectivity (for comparison, see the discussion above of selectivity of

heterobimetallic homogeneous hydrogenation catalysts). Thus, MgO-supported rhodium carbonyl pair-sites were found to have high selectivity for hydrogenation of 1,3-butadiene to give *n*-butenes (>99%) at both low and high conversions (Figure 9).[9b] The selectivity was improved by selectively poisoning the sites for terminal bonding of CO and slowly removing the bridging carbonyl ligands during catalytic operation, as mentioned above. The changes evidently led to limited H_2 dissociation and preferred bonding of the diene over the *n*-butene, which helped to limit sequential reactions and butane formation.

6.4. Iridium Pair-Site Catalysts for Water Oxidation. Zhao et al.[30] reported α-Fe_2O_3-supported catalysts made from a dimeric iridium complex with Ir–O–Ir bonds and multiple organic ligands, as mentioned above; adsorption of the precursor was followed by photochemical treatment to remove organic ligands, with the resulting surface species characterized by pairs of iridium atoms, shown in Figure 4. IR spectra of bridging CO ligands confirm the pair structure, with Ir–O–Ir bonds and not Ir–Ir bonds. The catalyst was tested for photochemical oxidation of water in the presence of an aqueous environment. The authors reported that the TOF characterizing the pair-site catalyst was five times that of a comparable single-site catalyst.

In related work by Zhao et al.,[65] a similar synthesis method was used to prepare WO_3-supported catalysts that the authors inferred on the basis of STEM and IR data bolstered by DFT calculations incorporated iridium pair-sites with end-on binding. These were used for photochemical oxidation of water in the presence of an aqueous environment. DFT calculations were used to investigate the water oxidation reaction catalyzed by the iridium pair-sites on both the Fe_3O_4 and WO_3 supports.[30, 65] In both of these investigations, the authors used the CHE approach to account for the applied electric potential. Significantly, although in the first report

with Fe_3O_4 the authors did not include the effect of solvation in their computational model, in the more recent work with WO_3 they accounted for solvation effects (implemented using the implicit solvation approach) and showed that they resulted in differences in the mechanism of Ir–O bond hydrolysis. This result suggests that inclusion of solvation effects is important in calculation of binding energies. It is likely that further work on the structural evolution of these materials in humid environments will benefit from inclusion of explicit calculations of reaction barriers in the presence of solvating environments.

7. CONCLUSIONS

The field of atomically precise supported metal pair-site catalysts is just emerging. Its progress depends on precise syntheses and accurate atomic-scale characterization. Most of the few examples of such catalysts have been made by anchoring molecular precursors with metal pairs onto supports or by precisely controlled aggregation of metal monomers on supports. A successful synthesis takes account of the ligands and metal–support interactions.

It is only through detailed characterization that it can be ascertained whether the synthesis of metal pair-sites has been successful. These methods must be transferred to *in-situ* or *in-operando* conditions to determine whether the structures are stable under catalytic conditions. There is no single method that can provide this critical structural information; it is only through a combination of experimental characterization methods, combined with theoretical calculations to aid in the interpretation, that we can have confidence in relating the performance of a catalyst to the presence of a metal pair-site. For methods such as XAS, a bulk averaging method, precise synthesis is a prerequisite to ensure that all of the metal atoms are present in pair sites, and thus

that the structural information can be interpreted directly. Likewise, for atomic-resolution electron microscopy methods, by which only a very small fraction of the material is imaged, it is essential that there be confirmation by XAS, which probes large amounts of material. Because supported metal pair-site catalysts have structures that are more nearly uniform than those of most solid catalysts, theory is especially valuable for prediction of reactivities and catalytic reaction mechanisms.

Metal pair-sites on supports, because they have neighboring metal centers, open pathways to catalyze many reactions that cannot be catalyzed by supported single-site catalysts. The neighboring metals may cooperate, providing bridging bonding sites for the reactants. In comparison with larger metal clusters, metal pair-site catalysts may have highly unsaturated structures that are highly active. However, comparisons between metal single-site, pair-site, and larger cluster catalysts are typically limited because the ligands are not the same and because the nuclearities of the catalysts are dynamic under reaction conditions. *In-situ* characterizations and theory can help to advance the understanding of the structure–catalytic property relationships. We foresee rich opportunities for metal pair-site catalysts in the confines of zeotype materials (described below), with possibilities for stabilization of the sites as well as catalytic cooperativity between the paired metal atoms. Such confinement effects have no parallels in homogeneous catalysis, but they do resemble those of the clefts and pockets that are often invoked in enzymatic catalysis.

8. SUGGESTED DIRECTIONS FOR FUTURE RESEARCH

In the following section, we offer suggestions for further research in supported metal pair-site catalysts. We emphasize such catalysts in zeotype materials, seeing especially rich opportunities. Consequently, this section includes substantial background information about that topic, but the other suggested research directions are presented only briefly.

8.1. Zeotype Support Frameworks as Templates for Metal Pair-Sites. Our goals in the following section are to address the possibility of synthesizing metal-pair sites in the small pores of zeotype materials and to consider such materials as an emerging class of catalysts that may benefit from confinement to facilitate cooperative catalysis involving the metal pair. Although this is a fast-moving research area, it is also one currently at the limits of state-of-the-art structure characterization. The reported materials are complex, because of the following: (i) they consist of mixtures of sites with various metal nuclearities, which are challenging to characterize; (ii) there is a need to observe metal pair-sites in reactive atmospheres to address the proposed dynamic formation mechanisms; and (iii) it is not yet feasible to do AC STEM imaging of many of the low-atomic-number metals that have been shown to have catalytic relevance (e.g., copper)—a limitation that is compounded by the strong susceptibility of zeotype materials to electron beam damage. These confounding effects make it difficult to synthesize and characterize samples in this category with the degree of structural definition that we used as a criterion for inclusion elsewhere in this Perspective. Consequently, we have kept this section short with the goal of motivating future work, in what in our judgement is clearly a fruitful area.

In the first decade of this century, catalysts containing copper-pair sites (e.g., Cu–O–Cu) in small pores of zeolites such as chabazite were inferred to be active for selective catalytic reduction (SCR) of NO_x[73] and methane oxidation to methanol.[74] Research in both of these areas

has burgeoned; what is evident is that the formation of the copper pair-site occurs dynamically and reversibly, with copper mobility under reaction conditions thought to be facilitated by ammonia (during SCR catalysis),[27] and proton-aided diffusion of hydrated copper ions (during methane oxidation catalysis).[75] Copper diffusion under both SCR and methane oxidation catalysis conditions is enhanced by a high zeolite aluminum to silicon ratios.[27, 75-76] The strong propensity for forming copper pairs in methane oxidation catalysts is exemplified by results with samples having low copper loadings—as low as 0.04 copper atoms/cage—so that there is only little probability of having multiple copper atoms within the a cage in the material as synthesized. It is also apparent that mixtures of copper species with various nuclearities form under reaction conditions,[77] as copper loadings >0.3 copper atoms per cage are reported to lead to copper nanoparticle formation in methane oxidation catalysts.[75]

These complexities have led to a lively, ongoing debate as to whether isolated,[76] dimeric,[74, 78] or trimeric[79] copper sites are responsible for methane activation and the observed methane-to-methanol conversion catalysis.

It is striking that models comprising copper sites of all three of these nuclearities have also been invoked recently, on separate occasions, to explain active-site structures of enzymes—for the same reaction.[1, 80] Understanding of these enzymes is complicated by the same issues of multiple speciation that characterize the synthetic zeotype catalysts. Something as seemingly innocuous as a standard purification wash preceding protein crystallization can alter this speciation significantly—leading to different conclusions between research groups.[80a]

Lessons learned from the paired-copper structure in the small pores of zeolites emphasize the importance of *in-situ* characterization—and characterization under catalytic reaction conditions—for determining the relevant active site structures.[77] It is clear that this field is evolving rapidly on both the biological and synthetic catalyst fronts—and that it will continue to benefit from state-of-the-art characterization advances that one day may permit visualization of the sites under catalytic reaction conditions by STEM or other microscopic methods (perhaps even cryoEM).

We see this as a fertile area for research that has the potential to expand into investigations of well-defined metal-pair sites for a variety of metals, in various confined environments (including those controlled by variation of aluminum speciation and confinement by selection of the zeotype framework), and we foresee catalysts with structural definitions meeting the more stringent criteria stated elsewhere this Perspective.

8.2. Brief Suggestions for Further Research on Supported Metal Pair-Site Catalysts.

8.2.1. Use Heterobimetallic Dimers with Organic Ligands as Precursors. These could be used to synthesize supported catalysts with pairs of different metal atoms, such as early and late transition metal atoms. Catalysts in this class could provide links to the examples of homogeneous bimetallic catalysis referred to above. A number of investigations have shown better performance of heterobimetallic catalysts than monometallic catalysts for reactions such as selective catalytic reduction of NO_x, ethylene hydroformylation, and electrochemical catalytic reactions.[81] However, it remains challenging to synthesize the active sites uniformly as dimers and to achieve exclusively structures with one metal atom bonded exclusively to one atom of the other metal. One should be cautious about relating pair-site structures to their catalytic

performance when the catalysts are non-uniform and contain undefined clusters or even larger particles.

8.2.2. Investigate Metal Pair-Sites on Metals. Find out what new catalytic properties they offer; characterization by scanning tunneling microscopy (STM) is appealing when the supports are metal single crystals, and it is not restricted to low-atomic-number metals. Comparisons between single-metal-atom and paired-metal-atom species on supports might emerge. How stable would these materials be?

8.2.3. Investigate Metal Pair-Sites on Model Metal Oxide Supports. These supports might include thin layers of a metal oxide (e.g., MgO) on single-crystal metals[22b] and single-crystal metal oxides themselves, such as ZnO and TiO_2. With such samples, researchers could take advantage of characterization methods used in ultrahigh vacuum surface science and do imaging by STM. From this perspective, the metal oxide can be more than just an isolated metal atom as in homogeneous catalysis, because it can be tailored to control the direction and amount of charge transfer to the supported metal in a way that lacks parallels in homogeneous catalysis—by changing the metal oxide carrier concentration. This point has been nicely demonstrated for both oxidation and hydrogenation catalysis for platinum supported on TiO_2 on basis of the well-established Schwab effect.[82]

8.2.4. Work with Sets of Three (and Four and ….) Metal Atoms on Supports. There are precedents for such samples that go back decades, for example, showing marked differences between isolated rhenium atoms on MgO and groups of three rhenium atoms on MgO, the latter formed from $H_3Re_3(CO)_{12}$.[83] When more than two metal atoms are present in a cluster or a grouping on a support, the metals can be present in various configurations, such as linear, triangular, or other 3-D structures. In the sub-nanometer size region, these configurations can be

strongly dependent on the coordination environment provided by the support and transform under reaction conditions. Investigations of families of metal clusters with small, controlled nuclearities could lead to understanding of effects of nuclearity and ligand environment in catalysis, but the challenges of synthesizing structurally uniform and stable samples are formidable.

8.2.5. Use Advances in XAS for Deeper Understanding of Metal Pair-Sites. As the field of metal pair-site catalysis develops, we posit that XAS will remain an essential characterization technique and foresee that advances in XAS data analysis (e.g., using neural networks[84]) will provide more rapid analysis and understanding of the structural stabilities under reaction conditions—with catalysts such as those described here being well suited for testing advances in XAS methodology. Further, greater confidence in structural models could be gained by closer coupling of DFT and EXAFS modeling. The use of real-time methods, coupled with direct feedback using machine-learning algorithms, during the catalyst synthesis could be used to guide the synthesis conditions to ensure that a specific metal pair-site is successfully synthesized.[85] More advanced XAS methods including partial-yield fluorescence detection (e.g., high-energy resolution fluorescence detection (HERFD) XAS) could be used to probe not only the structure of the metal pair-site, but also characterize the ligands on the catalytic center.[86] And coupling of XAS with complementary characterization methods (e.g., DRIFTS) could provide checks that multiple methods are probing the same structure.[87] In addition to the physical structure derived from modeling of XAS data, there are opportunities to use XANES to probe the electronic structures of pair sites and to compare the results with results characterizing comparable single-site materials. It is likely that *ab-initio* codes will be needed to obtain quantitative understanding of charge transfer and the local density of unoccupied states.

8.2.6. Use Advanced Data Collection and Analysis of STEM-EELS to Better Understand Metal Pair-Site Catalysts. The method is in prospect particularly helpful with respect to localized effects of the support and defect environment. A primary challenge for the success of these experiments is damage to the sample by the electron beam, which affects both the paired metal atoms and the support. These concerns are exacerbated when the supports are zeolites.[88] Much more efficient use of the electron dose would be enabled by the automatic identification of diatomic features of interest through computer vision techniques using methods developed for defect identification[89] and collection of spectroscopic data from only those areas. Furthermore, the EELS acquisition could be self-terminating on the basis of dynamic analysis of SNR in the experimental spectra through local low-rank denoising.[90] Analysis and interpretation of large-scale EELS maps can also be streamlined by application of neural network techniques for spectral feature prediction. These methods have been developed recently for XAS[91] and are adaptable to EELS, which is based on similar underlying physics, either through transfer learning or training of similar networks.

AUTHOR INFORMATION

Corresponding Author

*Bruce C. Gates, bcgates@ucdavis.edu

Author Contributions

The manuscript was written with contributions of all authors. All authors have given approval to the final version of the manuscript.

Funding Sources

EG and BCG were supported by the U.S. Department of Energy (DOE), Office of Science, Basic Energy Sciences (BES) grant DE-FG02-04ER15513. Stanford Synchrotron Radiation Lightsource (SSRL) of SLAC National Accelerator Laboratory is supported by BES under Contract No. DE-AC02-76SF00515. Co-ACCESS is supported by the BES Chemical Sciences, Geosciences, and Biosciences Division. Work at the Molecular Foundry was supported by BES under Contract No. DE-AC02-05CH11231. CXK and AK were supported by the U.S. DOE, Office of Science, BES grant DE-SC0020320. JC acknowledges additional support from the Presidential Early Career Award for Scientists and Engineers (PECASE) through the DOE.

REFERENCES

1. Balasubramanian, R.; Smith, S. M.; Rawat, S.; Yatsunyk, L. A.; Stemmler, T. L.; Rosenzweig, A. C., Oxidation of methane by a biological dicopper centre. *Nature* **2010,** *465* (7294), 115-119.

2. (a) Wilcox, D. E., Binuclear metallohydrolases. *Chem. Rev.* **1996,** *96* (7), 2435-2458; (b) Lindahl, P. A., Metal-metal bonds in biology. *J. Inorg. Biochem.* **2012,** *106* (1), 172-178.

3. Delferro, M.; Marks, T. J., Multinuclear Olefin Polymerization Catalysts. *Chem. Rev.* **2011,** *111* (3), 2450-2485.

4. (a) Kember, M. R.; Williams, C. K., Efficient magnesium catalysts for the copolymerization of epoxides and CO_2; using water to synthesize polycarbonate polyols. *J. Am. Chem. Soc.* **2012,** *134* (38), 15676-15679; (b) Kremer, A. B.; Mehrkhodavandi, P., Dinuclear catalysts for the ring opening polymerization of lactide. *Coord. Chem. Rev.* **2019,** *380*, 35-57.

5. (a) Wang, A. Q.; Li, J.; Zhang, T., Heterogeneous single-atom catalysis. *Nat. Rev. Chem.* **2018,** *2* (6), 65-81; (b) Cui, X. J.; Li, W.; Ryabchuk, P.; Junge, K.; Beller, M., Bridging homogeneous and heterogeneous catalysis by heterogeneous single-metal-site catalysts. *Nat. Catal.* **2019,** *2* (3), 277-277.

6. (a) Guan, E.; Gates, B. C., Stable Rhodium Pair Sites on MgO: Influence of Ligands and Rhodium Nuclearity on Catalysis of Ethylene Hydrogenation and H-D Exchange in the Reaction of H_2 with D_2. *ACS Catal.* **2018,** *8* (1), 482-487; (b) Yang, D.; Xu, P.; Guan, E.; Browning, N. D.; Gates, B. C., Rhodium pair-sites on magnesium oxide: Synthesis, characterization, and catalysis of ethylene hydrogenation. *J. Catal.* **2016,** *338*, 12-20.

7. (a) Yardimci, D.; Serna, P.; Gates, B. C., Surface-Mediated Synthesis of Dimeric Rhodium Catalysts on MgO: Tracking Changes in the Nuclearity and Ligand Environment of the Catalytically Active Sites by X-ray Absorption and Infrared Spectroscopies. *Chem-Eur. J.* **2013,** *19* (4), 1235-1245; (b) Yan, H.; Lin, Y.; Wu, H.; Zhang, W. H.; Sun, Z. H.; Cheng, H.; Liu, W.; Wang, C. L.; Li, J. J.; Huang, X. H.; Yao, T.; Yang, J. L.; Wei, S. Q.; Lu, J. L., Bottom-up precise synthesis of stable platinum dimers on graphene. *Nat. Commun.* **2017,** *8,* 1070.

8. (a) Buchwalter, P.; Rose, J.; Braunstein, P., Multimetallic Catalysis Based on Heterometallic Complexes and Clusters. *Chem. Rev.* **2015,** *115* (1), 28-126; (b) Kalck, P., Homo- and Heterobimetallic Complexes in Catalysis Cooperative Catalysis Preface. *Top. Organomet. Chem.* **2016,** *59*, 5-12; (c) Cooper, B. G.; Napoline, J. W.; Thomas, C. M., Catalytic Applications of Early/Late Heterobimetallic Complexes. *Catal. Rev. Sci. Eng.* **2012,** *54*, 1-40; (d) Thomas, C. M., Metal-Metal Multiple Bonds in Early/Late Heterobimetallic Complexes: Applications toward Small Molecule Activation and Catalysis. *Comment Inorg. Chem.* **2011,** *32*, 14-38; (e) Cammarota, R. C.; Clouston, L. J.; Lu, C. C., Leveraging molecular metal-support interactions for H_2 and N_2 activation. *Coord. Chem. Rev.* **2017,** *334*, 100-111; (f) Park, J.; Hong, S., Cooperative bimetallic catalysis in asymmetric transformations. *Chem. Soc. Rev.* **2012,** *41* (21), 6931-6943.

9. (a) Guan, E.; Debefve, L.; Vasiliu, M.; Zhang, S. J.; Dixon, D. A.; Gates, B. C., MgO-Supported Iridium Metal Pair-Site Catalysts Are More Active and Resistant to CO Poisoning than Analogous Single-Site Catalysts for Ethylene Hydrogenation and Hydrogen-Deuterium Exchange. *ACS Catal.* **2019,** *9* (10), 9545-9553; (b) Yardimci, D.; Serna, P.; Gates, B. C., Tuning Catalytic Selectivity: Zeolite- and Magnesium Oxide-Supported Molecular Rhodium Catalysts for Hydrogenation of 1,3-Butadiene. *ACS Catal.* **2012,** *2* (10), 2100-2113; (c) Tian, S. B.; Fu, Q.; Chen, W. X.; Feng, Q. C.; Chen, Z.; Zhang, J.; Cheong, W. C.; Yu, R.; Gu, L.; Dong,

J. C.; Luo, J.; Chen, C.; Peng, Q.; Draxl, C.; Wang, D. S.; Li, Y. D., Carbon nitride supported Fe_2 cluster catalysts with superior performance for alkene epoxidation. *Nat. Commun.* **2018,** *9,* 2353.

10. (a) Burch, R. R.; Muetterties, E. L.; Teller, R. G.; Williams, J. M., Selective Formation of Trans Olefins by a Catalytic-Hydrogenation of Alkynes Mediated at two Adjacent Metal Centers. *J. Am. Chem. Soc.* **1982,** *104* (15), 4257-4258; (b) Burch, R. R.; Shusterman, A. J.; Muetterties, E. L.; Teller, R. G.; Williams, J. M., Coordinately Unsaturated Clusters - a Novel Catalytic Reaction. *J. Am. Chem. Soc.* **1983,** *105* (11), 3546-3556.

11. Muetterties, E. L., Selective Reactions of Transition-Metals and Their Complexes. *Inorg. Chim. Acta* **1981,** *50* (1), 1-9.

12. Schleyer, D.; Niessen, H. G.; Bargon, J., In situ ^{1}H-PHIP-NMR studies of the stereoselective hydrogenation of alkynes to (*E*)-alkenes catalyzed by a homogeneous $[Cp^*Ru]^+$ catalyst. *New J. Chem.* **2001,** *25* (3), 423-426.

13. Hostetler, M. J.; Bergman, R. G., Synthesis and Reactivity of $Cp_2Ta(CH_2)_2Ir(CO)_2$: An Early-Late Heterobimetallic Complex That Catalytically Hydrogenates, Isomerizes, and Hydrosilates Alkenes. *J. Am. Chem. Soc.* **1990,** *112* (23), 8621-8623.

14. Ferguson, G. S.; Wolczanski, P. T.; Parkanyi, L.; Zonnevylle, M. C., Synthesis and Reactivity of Heterobimetallic "A-Frames" and Rh-Zr Bonded Complexes: Structure of $Cp^*Zr(\mu\text{-}OCH_2Ph_2P)_2RhMe_2$. *Organometallics* **1988,** *7* (9), 1967-1979.

15. (a) Hanna, T. A.; Baranger, A. M.; Bergman, R. G., Reaction of Carbon-Dioxide and Heterocumulenes with an Unsymmetrical Metal-Metal Bond - Direct Addition of Carbon-Dioxide across a Zirconium-Iridium Bond and Stoichiometric Reduction of Carbon-Dioxide to Formate. *J. Am. Chem. Soc.* **1995,** *117* (45), 11363-11364; (b) Pinkes, J. R.; Steffey, B. D.; Vites, J. C.; Cutler, A. R., Carbon Dioxide Insertion into the Fe-Zr and Ru-Zr Bonds of the Heterobimetallic Complexes $Cp(CO)_2M\text{-}Zr(Cl)Cp_2$: Direct Production of the $\mu\text{-}\eta^1(C):\eta^2(O,O')\text{-}CO_2$ Compounds $Cp(CO)_2M\text{-}CO_2\text{-}Zr(Cl)Cp_2$. *Organometallics* **1994,** *13* (1), 21-23; (c) Memmler, H.; Kauper, U.; Gade, L. H.; Scowen, I. J.; McPartlin, M., Insertion of X=C=Y heteroallenes into unsupported Zr-M bonds (M = Fe, Ru). *Chem. Commun.* **1996,** (15), 1751-1752.

16. Zhou, W.; Napoline, J. W.; Thomas, C. M., A Catalytic Application of Co/Zr Heterobimetallic Complexes: Kumada Coupling of Unactivated Alkyl Halides with Alkyl Grignard Reagents. *Eur. J. Inorg. Chem.* **2011,** (13), 2029-2033.

17. Cammarota, R. C.; Vollmer, M. V.; Xie, J.; Ye, J. Y.; Linehan, J. C.; Burgess, S. K.; Appel, A. M.; Gagliardi, L.; Lu, C. C., A Bimetallic Nickel-Gallium Complex Catalyzes CO_2 Hydrogenation via the Intermediacy of an Anionic d^{10} Nickel Hydride. *J. Am. Chem. Soc.* **2017,** *139* (40), 14244-14250.

18. Cammarota, R. C.; Lu, C. C., Tuning Nickel with Lewis Acidic Group 13 Metalloligands for Catalytic Olefin Hydrogenation. *J. Am. Chem. Soc.* **2015,** *137* (39), 12486-12489.

19. Schneider, H. J.; Schmidt, G.; Thomas, F., Alicyclic reaction mechanisms. 6. Strain-reactivity relations as a tool for the localization of transition states. Equilibria, solvolysis, and redox reactions of substituted cycloalkanes. *J. Am. Chem. Soc.* **1983,** *105* (11), 3556-3563.

20. Desai, S. P.; Ye, J.; Zheng, J.; Ferrandon, M. S.; Webber, T. E.; Platero-Prats, A. E.; Duan, J. X.; Garcia-Holley, P.; Camaioni, D. M.; Chapman, K. W.; Delferro, M.; Farha, O. K.; Fulton, J. L.; Gagliardi, L.; Lercher, J. A.; Penn, R. L.; Stein, A.; Lu, C. C., Well-Defined Rhodium-Gallium Catalytic Sites in a Metal-Organic Framework: Promoter-Controlled Selectivity in Alkyne Semihydrogenation to *E*-Alkenes. *J. Am. Chem. Soc.* **2018,** *140* (45), 15309-15318.

21. (a) Schenck, T. G.; Milne, C. R. C.; Sawyer, J. F.; Bosnich, B., Bimetallic Reactivity - Oxidative-Addition and Reductive-Elimination Reactions of Rhodium and Iridium Bimetallic Complexes. *Inorg. Chem.* **1985,** *24* (15), 2338-2344; (b) Gade, L. H.; Memmler, H.; Kauper, U.; Schneider, A.; Fabre, S.; Bezougli, I.; Lutz, M.; Galka, C.; Scowen, I. J.; McPartlin, M., Cooperative reactivity of early-late heterodinuclear transition metal complexes with polar organic substrates. *Chem. Eur. J.* **2000,** *6* (4), 692-708.

22. (a) Papile, C. J.; Knözinger, H.; Gates, B. C., $[Re_2(CO)_9]^{2-}$ on hydroxylated MgO: Formation from $[Re_2(CO)_{10}]$ and evidence of ion pairing at the surface. *Langmuir* **2000,** *16* (13), 5661-5664; (b) Purnell, S. K.; Xu, X.; Goodman, D. W.; Gates, B. C., Adsorption and Reaction of $[Re_2(CO)_{10}]$ on Ultrathin MgO Films Grown on a Mo(110) Surface - Characterization by Infrared Reflection-Absorption Spectroscopy and Temperature-Programmed Desorption. *J. Phys. Chem.* **1994,** *98* (15), 4076-4082.

23. Bando, K. K.; Asakura, K.; Arakawa, H.; Isobe, K.; Iwasawa, Y., Surface structures and catalytic hydroformylation activities of Rh dimers attached on various inorganic oxide supports. *J. Phys. Chem.* **1996,** *100* (32), 13636-13645.

24. (a) Whyman, R., Dirhodium octacarbonyl. *Chem. Commun.* **1970,** (18), 1194-1195; (b) Hanlan, L. A.; Ozin, G. A., Synthesis Using Transition-Metal Diatomic-Molecules - Dirhodium Octacarbonyl, $Rh_2(CO)_8$, and Diiridium Octacarbonyl, $Ir_2(CO)_8$. *J. Am. Chem. Soc.* **1974,** *96* (20), 6324-6329.

25. Theolier, A.; Smith, A. K.; Leconte, M.; Basset, J. M.; Zanderighi, G. M.; Psaro, R.; Ugo, R., Surface Supported Metal Cluster Carbonyls - Chemisorption Decomposition and Reactivity of $Rh_4(CO)_{12}$ Supported on Silica and Alumina. *J. Organomet. Chem.* **1980,** *191* (2), 415-424.

26. (a) Wichterlova, B.; Sobalik, Z.; Dědeček, J., Cu ion siting in high silica zeolites. Spectroscopy and redox properties. *Catal. Today* **1997,** *38* (2), 199-203; (b) Chavan, S.; Srinivas, D.; Ratnasamy, P., Structure and catalytic properties of dimeric copper(II) acetato complexes encapsulated in zeolite-Y. *J. Catal.* **2000,** *192* (2), 286-295; (c) Asakura, K.; Noguchi, Y.; Iwasawa, Y., Stepwise synthesis and structure analysis of Mo dimers in NaY zeolite. *J. Phys. Chem. B* **1999,** *103* (7), 1051-1058; (d) Yakovlev, A. L.; Shubin, A. A.; Zhidomirov, G. M.; van Santen, R. A., DFT study of oxygen-bridged Zn^{2+} ion pairs in Zn/ZSM-5 zeolites. *Catal. Lett.* **2000,** *70* (3-4), 175-181.

27. Paolucci, C.; Khurana, I.; Parekh, A. A.; Li, S. C.; Shih, A. J.; Li, H.; Di Iorio, J. R.; Albarracin-Caballero, J. D.; Yezerets, A.; Miller, J. T.; Delgass, W. N.; Ribeiro, F. H.; Schneider, W. F.; Gounder, R., Dynamic multinuclear sites formed by mobilized copper ions in NO_x selective catalytic reduction. *Science* **2017,** *357* (6354), 898-903.

28. Schöttle, C.; Guan, E.; Okrut, A.; Grosso-Giordano, N. A.; Palermo, A.; Solovyov, A.; Gates, B. C.; Katz, A., Bulky Calixarene Ligands Stabilize Supported Iridium Pair-Site Catalysts. *J. Am. Chem. Soc.* **2019,** *141* (9), 4010-4015.

29. Asakura, K.; Kitamurabando, K.; Iwasawa, Y.; Arakawa, H.; Isobe, K., Metal-Assisted Hydroformylation on a SiO_2-Attached Rh Dimer - In situ EXAFS and FTIR Observations of the Dynamic Behaviors of the Dimer Site. *J. Am. Chem. Soc.* **1990,** *112* (25), 9096-9104.

30. Zhao, Y. Y.; Yang, K. R.; Wang, Z. C.; Yan, X. X.; Cao, S. F.; Ye, Y. F.; Dong, Q.; Zhang, X. Z.; Thorne, J. E.; Jin, L.; Materna, K. L.; Trimpalis, A.; Bai, H. Y.; Fakra, S. C.; Zhong, X.

Y.; Wang, P.; Pan, X. Q.; Guo, J. H.; Flytzani-Stephanopoulos, M.; Brudvig, G. W.; Batista, V. S.; Wang, D. W., Stable iridium dinuclear heterogeneous catalysts supported on metal-oxide substrate for solar water oxidation. *Proc. Nat. Acad. Sci. USA* **2018,** *115* (12), 2902-2907.

31. DeRita, L.; Resasco, J.; Dai, S.; Boubnov, A.; Thang, H. V.; Hoffman, A. S.; Ro, I.; Graham, G. W.; Bare, S. R.; Pacchioni, G.; Pan, X. Q.; Christopher, P., Structural evolution of atomically dispersed Pt catalysts dictates reactivity. *Nat. Mater.* **2019,** *18* (7), 746-751.

32. Yang, D.; Xu, P.; Browning, N. D.; Gates, B. C., Tracking Rh Atoms in Zeolite HY: First Steps of Metal Cluster Formation and Influence of Metal Nuclearity on Catalysis of Ethylene Hydrogenation and Ethylene Dimerization. *J. Phys. Chem. Lett.* **2016,** *7* (13), 2537-2543.

33. (a) Smeets, P. J.; Hadt, R. G.; Woertink, J. S.; Vanelderen, P.; Schoonheydt, R. A.; Sels, B. F.; Solomon, E. I., Oxygen Precursor to the Reactive Intermediate in Methanol Synthesis by Cu-ZSM-5. *J. Am. Chem. Soc.* **2010,** *132* (42), 14736-14738; (b) Vanelderen, P.; Snyder, B. E. R.; Tsai, M. L.; Hadt, R. G.; Vancauwenbergh, J.; Coussens, O.; Schoonheydt, R. A.; Sels, B. F.; Solomon, E. I., Spectroscopic Definition of the Copper Active Sites in Mordenite: Selective Methane Oxidation. *J. Am. Chem. Soc.* **2015,** *137* (19), 6383-6392.

34. S. F. Kurtoğlu, A. S. H., D. Akgül, M. Babucci, V. Aviyente, B. C. Gates, S. R. Bare, and A. Uzun. , Electronic Structure of Atomically Dispersed Supported Iridium Catalyst Controls Iridium Aggregation. *Unpublished results*.

35. Hamzaoui, B.; Pelletier, J. D. A.; Abou-Hamad, E.; Chen, Y.; El Eter, M.; Chermak, E.; Cavallo, L.; Basset, J.-M., Solid-State NMR and DFT Studies on the Formation of Well-Defined Silica-Supported Tantallaaziridines: From Synthesis to Catalytic Application. *Chem. Eur. J.* **2016,** *22* (9), 3000-3008.

36. (a) Qiao, B. T.; Wang, A. Q.; Yang, X. F.; Allard, L. F.; Jiang, Z.; Cui, Y. T.; Liu, J. Y.; Li, J.; Zhang, T., Single-atom catalysis of CO oxidation using Pt_1/FeO_x. *Nat. Chem.* **2011,** *3* (8), 634-641; (b) Liu, J. Y., Catalysis by Supported Single Metal Atoms. *ACS Catal.* **2017,** *7* (1), 34-59; (c) Liu, J. J.; Xu, J.; Lou, Y.; Cai, Y.; Li, X., Anchoring and Localizing Single Metal Atoms for Better Catalysis. *Microsc. Microanal.* **2018,** *24*, 20-21; (d) Debefve, L. M.; Hoffinan, A. S.; Yeh, A. J.; Runnebaum, R. C.; Shulda, S.; Richards, R. M.; Arslan, I.; Gates, B. C., Iridium Atoms Bonded to Crystalline Powder MgO: Characterization by Imaging and Spectroscopy. *J. Phys. Chem. C* **2020,** *124* (1), 459-468.

37. Wang, J.; Huang, Z. Q.; Liu, W.; Chang, C. R.; Tang, H. L.; Li, Z. J.; Chen, W. X.; Jia, C. J.; Yao, T.; Wei, S. Q.; Wu, Y.; Lie, Y. D., Design of N-Coordinated Dual-Metal Sites: A Stable and Active Pt-Free Catalyst for Acidic Oxygen Reduction Reaction. *J. Am. Chem. Soc.* **2017,** *139* (48), 17281-17284.

38. Nemana, S.; Sun, J.; Gates, B. C., Reactivity of binuclear tantalum clusters on silica: Characterization by transient time-resolved spectroscopy. *J. Phys. Chem. C* **2008,** *112* (19), 7477-7485.

39. (a) Colliex, C.; Gloter, A.; March, K.; Mory, C.; Stéphan, O.; Suenaga, K.; Tencé, M., Capturing the signature of single atoms with the tiny probe of a STEM. *Ultramicroscopy* **2012,** *123*, 80-89; (b) Krivanek, O. L.; Dellby, N.; Murfitt, M. F.; Chisholm, M. F.; Pennycook, T. J.; Suenaga, K.; Nicolosi, V., Gentle STEM: ADF imaging and EELS at low primary energies. *Ultramicroscopy* **2010,** *110* (8), 935-945.

40. Suenaga, K.; Koshino, M., Atom-by-atom spectroscopy at graphene edge. *Nature* **2010,** *468* (7327), 1088-1090.

41. Senga, R.; Suenaga, K., Single-atom electron energy loss spectroscopy of light elements. *Nat. Commun.* **2015,** *6* (1), 7943.

42. Hage, F. S.; Radtke, G.; Kepaptsoglou, D. M.; Lazzeri, M.; Ramasse, Q. M., Single-atom vibrational spectroscopy in the scanning transmission electron microscope. *Science* **2020,** *367* (6482), 1124-1127.

43. Egerton, R. F.; Watanabe, M., Characterization of single-atom catalysts by EELS and EDX spectroscopy. *Ultramicroscopy* **2018,** *193*, 111-117.

44. Aydin, C.; Lu, J.; Browning, N. D.; Gates, B. C., A "Smart" Catalyst: Sinter-Resistant Supported Iridium Clusters Visualized with Electron Microscopy. *Angew. Chem. Int. Ed.* **2012,** *51* (24), 5929-5934.

45. Cao, K.; Skowron, S. T.; Biskupek, J.; Stoppiello, C. T.; Leist, C.; Besley, E.; Khlobystov, A. N.; Kaiser, U., Imaging an unsupported metal–metal bond in dirhenium molecules at the atomic scale. *Sci. Advan.* **2020,** *6* (3), 5849.

46. van Oversteeg, C. H. M.; Doan, H. Q.; de Groot, F. M. F.; Cuk, T., In situ X-ray absorption spectroscopy of transition metal based water oxidation catalysts. *Chem. Soc. Rev.* **2017,** *46* (1), 102-125.

47. Hadjiivanov, K. I.; Vayssilov, G. N., Characterization of oxide surfaces and zeolites by carbon monoxide as an IR probe molecule. *Adv. Catal.* **2002,** *47*, 307-511.

48. Bhirud, V. A.; Ehresmann, J. O.; Kletnieks, P. W.; Haw, J. F.; Gates, B. C., Rhodium complex with ethylene ligands supported on highly dehydroxylated MgO: Synthesis, characterization, and reactivity. *Langmuir* **2006,** *22* (1), 490-496.

49. Hoffman, A. S.; Fang, C. Y.; Gates, B. C., Homogeneity of Surface Sites in Supported Single-Site Metal Catalysts: Assessment with Band Widths of Metal Carbonyl Infrared Spectra. *J. Phys. Chem. Lett.* **2016,** *7* (19), 3854-3860.

50. (a) Salmeron, M.; Schlogl, R., Ambient pressure photoelectron spectroscopy: A new tool for surface science and nanotechnology. *Surf Sci Rep* **2008,** *63* (4), 169-199; (b) Nguyen, L.; Tao, F. F.; Tang, Y.; Doug, J.; Bao, X. J., Understanding Catalyst Surfaces during Catalysis through Near Ambient Pressure X-ray Photoelectron Spectroscopy. *Chem. Rev.* **2019,** *119* (12), 6822-6905.

51. Lykhach, Y.; Figueroba, A.; Camellone, M. F.; Neitzel, A.; Skala, T.; Negreiros, F. R.; Vorokhta, M.; Tsud, N.; Prince, K. C.; Fabris, S.; Neyman, K. M.; Matolin, V.; Libuda, J., Reactivity of atomically dispersed Pt^{2+} species towards H_2: model Pt-CeO_2 fuel cell catalyst. *Phys. Chem. Chem. Phys.* **2016,** *18* (11), 7672-7679.

52. Tada, M.; Sasaki, T.; Shido, T.; Iwasawa, Y., Design, characterization and performance of a molecular imprinting Rh-dimer hydrogenation catalyst on a SiO_2 surface. *Phys. Chem. Chem. Phys.* **2002,** *4* (23), 5899-5909.

53. Okada, K.; Kotani, A., Complementary Roles of Co 2p X-Ray Absorption and Photoemission Spectra in CoO. *J. Phys. Soc. Jpn.* **1992,** *61* (2), 449-453.

54. Stroscio, J. A.; Kaiser, W. J., *Scanning tunneling microscopy*. Academic press: 1993; Vol. 27, 298.

55. Bartels, L.; Meyer, G.; Rieder, K. H., Controlled vertical manipulation of single CO molecules with the scanning tunneling microscope: A route to chemical contrast. *Appl. Phys. Lett.* **1997,** *71* (2), 213-215.

56. (a) Evans, M. M. R.; Nogami, J., Indium and gallium on Si(001): A closer look at the parallel dimer structure. *Phys. Rev. B* **1999,** *59* (11), 7644-7648; (b) Itoh, H.; Itoh, J.; Schmid, A.;

Ichinokawa, T., Structures of Low-Coverage Phases of Al on the Si(100) Surface Observed by Scanning-Tunneling-Microscopy. *Phys. Rev. B* **1993,** *48* (19), 14663-14666.

57. Sobotik, P.; Setvin, M.; Zimmermann, P.; Kocan, P.; Ost'adal, I.; Mutombo, P.; Ondracek, M.; Jelinek, P., Emergence of state at Fermi level due to the formation of In-Sn heterodimers on Si(100)-2 x 1. *Phys. Rev. B* **2013,** *88* (20), 205406.

58. Anisimov, V. I.; Aryasetiawan, F.; Lichtenstein, A. I., First-principles calculations of the electronic structure and spectra of strongly correlated systems: The LDA+U method. *J. Phys.-Condens. Mat.* **1997,** *9* (4), 767-808.

59. (a) Mandal, S.; Haule, K.; Rabe, K. M.; Vanderbilt, D., Systematic beyond-DFT study of binary transition metal oxides. *Npj Comput. Mater.* **2019,** *5*, 115; (b) Perdew, J. P.; Zunger, A., Self-Interaction Correction to Density-Functional Approximations for Many-Electron Systems. *Phys. Rev. B* **1981,** *23* (10), 5048-5079.

60. Stevanović, V.; Lany, S.; Zhang, X. W.; Zunger, A., Correcting density functional theory for accurate predictions of compound enthalpies of formation: Fitted elemental-phase reference energies. *Phys. Rev. B* **2012,** *85*, 115104.

61. Cao, K. C.; Skowron, S. T.; Biskupek, J.; Stoppiello, C. T.; Leist, C.; Besley, E.; Khlobystov, A. N.; Kaiser, U., Imaging an unsupported metal-metal bond in dirhenium molecules at the atomic scale. *Sci. Adv.* **2020,** *6* (3), 5849.

62. Borin, A. C.; Gobbo, J. P.; Roos, B. O., Electronic structure and chemical bonding in the ground states of Tc-2 and Re-2. *Mol. Phys.* **2009,** *107* (8-12), 1035-1040.

63. (a) Nørskov, J. K.; Rossmeisl, J.; Logadottir, A.; Lindqvist, L.; Kitchin, J. R.; Bligaard, T.; Jonsson, H., Origin of the overpotential for oxygen reduction at a fuel-cell cathode. *J. Phys. Chem. B* **2004,** *108* (46), 17886-17892; (b) Kulkarni, A.; Siahrostami, S.; Patel, A.; Nørskov, J. K., Understanding Catalytic Activity Trends in the Oxygen Reduction Reaction. *Chem. Rev.* **2018,** *118* (5), 2302-2312.

64. Scott, A. P.; Radom, L., Harmonic vibrational frequencies: An evaluation of Hartree-Fock, Moller-Plesset, quadratic configuration interaction, density functional theory, and semiempirical scale factors. *J. Phys. Chem.* **1996,** *100* (41), 16502-16513.

65. Zhao, Y. Y.; Yan, X. X.; Yang, K. R.; Cao, S. F.; Dong, Q.; Thorne, J. E.; Materna, K. L.; Zhu, S. S.; Pan, X. Q.; Flytzani-Stephanopoulos, M. F.; Brudvig, G. W.; Batista, V. S.; Wang, D.

W., End-On Bound Iridium Dinuclear Heterogeneous Catalysts on WO_3 for Solar Water Oxidation. *ACS Cent. Sci.* **2018,** *4* (9), 1166-1172.

66. Piccini, G.; Sauer, J., Effect of Anharmonicity on Adsorption Thermodynamics. *J Chem Theory Comput.* **2014,** *10* (6), 2479-2487.

67. Zhai, H.; Alexandrova, A. N., Fluxionality of Catalytic Clusters: When It Matters and How to Address It. *ACS Catal.* **2017,** *7* (3), 1905-1911.

68. Lu, J.; Serna, P.; Gates, B. C., Zeolite- and MgO-Supported Molecular Iridium Complexes: Support and Ligand Effects in Catalysis of Ethene Hydrogenation and H-D Exchange in the Conversion of H_2+D_2. *ACS Catal.* **2011,** *1* (11), 1549-1561.

69. (a) Tsung, C. K.; Kuhn, J. N.; Huang, W. Y.; Aliaga, C.; Hung, L. I.; Somorjai, G. A.; Yang, P. D., Sub-10 nm Platinum Nanocrystals with Size and Shape Control: Catalytic Study for Ethylene and Pyrrole Hydrogenation. *J. Am. Chem. Soc.* **2009,** *131* (16), 5816-5822; (b) Marsh, A. L.; Somorjai, G. A., Structure, reactivity, and mobility of carbonaceous overlayers during olefin hydrogenation on platinum and rhodium single crystal surfaces. *Top. Catal.* **2005,** *34*, 121-128; (c) Mitsui, T.; Rose, M. K.; Fomin, E.; Ogletree, D. F.; Salmeron, M., Dissociative hydrogen adsorption on palladium requires aggregates of three or more vacancies. *Nature* **2003,** *422* (6933), 705-707.

70. Cortright, R. D.; Goddard, S. A.; Rekoske, J. E.; Dumesic, J. A., Kinetic-Study of Ethylene Hydrogenation. *J. Catal.* **1991,** *127* (1), 342-353.

71. Ren, H.; Humbert, M. P.; Menning, C. A.; Chen, J. G.; Shu, Y. Y.; Singh, U. G.; Cheng, W. C., Inhibition of coking and CO poisoning of Pt catalysts by the formation of Au/Pt bimetallic surfaces. *Appl. Catal. A-Gen.* **2010,** *375* (2), 303-309.

72. Liu, J. L.; Lucci, F. R.; Yang, M.; Lee, S.; Marcinkowski, M. D.; Therrien, A. J.; Williams, C. T.; Sykes, E. C. H.; Flytzani-Stephanopoulos, M., Tackling CO Poisoning with Single-Atom Alloy Catalysts. *J. Am. Chem. Soc.* **2016,** *138* (20), 6396-6399.

73. Bull, I.; Xue, W.-M.; Burk, P.; Boorse, R. S.; Jaglowski, W. M.; Koermer, G. S.; Moini, A.; Patchett, J. A.; Dettling, J. C.; Caudle, M. T., Copper CHA zeolite catalysts. US Patent 7,601,662, **2009**.

74. Groothaert, M. H.; Smeets, P. J.; Sels, B. F.; Jacobs, P. A.; Schoonheydt, R. A., Selective oxidation of methane by the bis(mu-oxo)dicopper core stabilized on ZSM-5 and mordenite zeolites. *J. Am. Chem. Soc.* **2005,** *127* (5), 1394-1395.

75. Dinh, K. T.; Sullivan, M. M.; Narsimhan, K.; Serna, P.; Meyer, R. J.; Dinca, M.; Roman-Leshkov, Y., Continuous Partial Oxidation of Methane to Methanol Catalyzed by Diffusion-Paired Copper Dimers in Copper-Exchanged Zeolites. *J. Am. Chem. Soc.* **2019,** *141* (29), 11641-11650.

76. Pappas, D. K.; Borfecchia, E.; Dyballa, M.; Pankin, I. A.; Lomachenko, K. A.; Martini, A.; Signorile, M.; Teketel, S.; Arstad, B.; Berlier, G.; Lamberti, C.; Bordiga, S.; Olsbye, U.; Lillerud, K. P.; Svelle, S.; Beato, P., Methane to Methanol: Structure Activity Relationships for Cu-CHA. *J. Am. Chem. Soc.* **2017,** *139* (42), 14961-14975.

77. Newton, M. A.; Knorpp, A. J.; Sushkevich, V. L.; Palagin, D.; van Bokhoven, J. A., Active sites and mechanisms in the direct conversion of methane to methanol using Cu in zeolitic hosts: a critical examination. *Chem. Soc. Rev.* **2020,** *49* (5), 1449-1486.

78. Groothaert, M. H.; van Bokhoven, J. A.; Battiston, A. A.; Weckhuysen, B. M.; Schoonheydt, R. A., Bis(mu-oxo)dicopper in Cu-ZSM-5 and its role in the decomposition of NO: A combined in situ XAFS, UV-Vis-Near-IR, and kinetic study. *J. Am. Chem. Soc.* **2003,** *125* (25), 7629-7640.

79. (a) Grundner, S.; Markovits, M. A. C.; Li, G.; Tromp, M.; Pidko, E. A.; Hensen, E. J. M.; Jentys, A.; Sanchez-Sanchez, M.; Lercher, J. A., Single-site trinuclear copper oxygen clusters in mordenite for selective conversion of methane to methanol. *Nat. Commun.* **2015,** *6*, 7546; (b) Li, G. N.; Vassilev, P.; Sanchez-Sanchez, M.; Lercher, J. A.; Hensen, E. J. M.; Pidko, E. A., Stability and reactivity of copper oxo-clusters in ZSM-5 zeolite for selective methane oxidation to methanol. *J. Catal.* **2016,** *338*, 305-312; (c) Grundner, S.; Luo, W.; Sanchez-Sanchez, M.; Lercher, J. A., Synthesis of single-site copper catalysts for methane partial oxidation. *Chem. Commun.* **2016,** *52* (12), 2553-2556.

80. (a) Chan, S. I.; Wang, V. C. C.; Lai, J. C. H.; Yu, S. S. F.; Chen, P. P. Y.; Chen, K. H. C.; Chen, C. L.; Chan, M. K., Redox potentiometry studies of particulate methane monooxygenase: Support for a trinuclear copper cluster active site. *Angew. Chem. Int. Ed.* **2007,** *46* (12), 1992-1994; (b) Ross, M. O.; MacMillan, F.; Wang, J. Z.; Nisthal, A.; Lawton, T. J.; Olafson, B. D.;

Mayo, S. L.; Rosenzweig, A. C.; Hoffman, B. M., Particulate methane monooxygenase contains only mononuclear copper centers. *Science* **2019,** *364* (6440), 566-570.

81. (a) Qu, W.; Liu, X.; Chen, J.; Dong, Y.; Tang, X.; Chen, Y., Single-atom catalysts reveal the dinuclear characteristic of active sites in NO selective reduction with NH_3. *Nat. Commun.* **2020,** *11* (1), 1-7; (b) Ro, I.; Xu, M.; Graham, G. W.; Pan, X.; Christopher, P., Synthesis of Heteroatom Rh–ReO x Atomically Dispersed Species on Al_2O_3 and Their Tunable Catalytic Reactivity in Ethylene Hydroformylation. *ACS Catal.* **2019,** *9* (12), 10899-10912; (c) Zhang, L.; Si, R.; Liu, H.; Chen, N.; Wang, Q.; Adair, K.; Wang, Z.; Chen, J.; Song, Z.; Li, J., Atomic layer deposited Pt-Ru dual-metal dimers and identifying their active sites for hydrogen evolution reaction. *Nat. Commun.* **2019,** *10* (1), 1-11.

82. (a) Gunasooriya, G. T. K. K.; Seebauer, E. G.; Saeys, M., Ethylene Hydrogenation over Pt/TiO_2: A Charge-Sensitive Reaction. *ACS Catal.* **2017,** *7* (3), 1966-1970; (b) Chua, Y. P. G.; Gunasooriya, G. T. K. K.; Saeys, M.; Seebauer, E. G., Controlling the CO oxidation rate over Pt/TiO_2 catalysts by defect engineering of the TiO_2 support. *J. Catal.* **2014,** *311*, 306-313.

83. (a) Kirlin, P.; Knözinger, H.; Gates, B. C., Mononuclear, trinuclear, and metallic rhenium catalysts supported on magnesia: effects of structure on catalyst performance. *J. Phys. Chem.* **1990,** *94* (22), 8451-8456; (b) Kirlin, P. S.; Gates, B. C., Activation of the C-C Bond Provides a Molecular-Basis for Structure Sensitivity in Metal Catalysis. *Nature* **1987,** *325* (6099), 38-40; (c) Kirlin, P. S.; Vanzon, F. B. M.; Koningsberger, D. C.; Gates, B. C., Surface Catalytic Sites Prepared from $[HRe(CO)_5]$ and $[H_3Re_3(CO)_{12}]$ - Mononuclear, Trinuclear, and Metallic Rhenium Catalysts Supported on MgO. *J. Phys. Chem.* **1990,** *94* (22), 8439-8450.

84. Timoshenko, J.; Anspoks, A.; Cintins, A.; Kuzmin, A.; Purans, J.; Frenkel, A. I., Neural Network Approach for Characterizing Structural Transformations by X-Ray Absorption Fine Structure Spectroscopy. *Phys. Rev. Lett.* **2018,** *120*, 225502.

85. Wu, L. H.; Lian, H. D.; Wills, J. J.; Goodman, E. D.; McKay, I. S.; Qin, J.; Tassone, C. J.; Cargnello, M., Tuning Precursor Reactivity toward Nanometer-Size Control in Palladium Nanoparticles Studied by in Situ Small Angle X-ray Scattering. *Chem. Mater.* **2018,** *30* (3), 1127-1135.

86. (a) Hoffman, A. S.; Sokaras, D.; Zhang, S. J.; Debefve, L. M.; Fang, C. Y.; Gallo, A.; Kroll, T.; Dixon, D. A.; Bare, S. R.; Gates, B. C., High-Energy-Resolution X-ray Absorption

Spectroscopy for Identification of Reactive Surface Species on Supported Single-Site Iridium Catalysts. *Chem. Eur. J.* **2017,** *23* (59), 14760-14768; (b) Lu, Y. B.; Wang, J. M.; Yu, L.; Kovarik, L.; Zhang, X. W.; Hoffman, A. S.; Gallo, A.; Bare, S. R.; Sokaras, D.; Kroll, T.; Dagle, V.; Xin, H. L.; Karim, A. M., Identification of the active complex for CO oxidation over single-atom Ir-on-$MgAl_2O_4$ catalysts. *Nat. Catal.* **2019,** *2* (2), 149-156.

87. Brieger, C.; Melke, J.; van der Bosch, N.; Reinholz, U.; Riesemeier, H.; Buzanich, A. G.; Kayarkatte, M. K.; Derr, I.; Schokel, A.; Roth, C., A combined in-situ XAS-DRIFTS study unraveling adsorbate induced changes on the Pt nanoparticle structure. *J. Catal.* **2016,** *339*, 57-67.

88. Mayoral, A.; Anderson, P. A.; Diaz, I., Zeolites are no longer a challenge: Atomic resolution data by Aberration-corrected STEM. *Micron* **2015,** *68*, 146-151.

89. Maksov, A.; Dyck, O.; Wang, K.; Xiao, K.; Geohegan, D. B.; Sumpter, B. G.; Vasudevan, R. K.; Jesse, S.; Kalinin, S. V.; Ziatdinov, M., Deep learning analysis of defect and phase evolution during electron beam-induced transformations in WS_2. *Npj Comput. Mater.* **2019,** *5*, 12.

90. Spiegelberg, J.; Idrobo, J. C.; Herklotz, A.; Ward, T. Z.; Zhou, W.; Rusz, J., Local low rank denoising for enhanced atomic resolution imaging. *Ultramicroscopy* **2018,** *187*, 34-42.

91. Carbone, M. R.; Topsakal, M.; Lu, D. Y.; Yoo, S., Machine-Learning X-Ray Absorption Spectra to Quantitative Accuracy. *Phys. Rev. Lett.* **2020,** *124*, 156401.